How have Cretan rivers responded to late Holocene uplift?

Macklin, Mark; Booth, Jonathan; Brewer, Paul; Tooth, Stephen; Duller, G. A. T.

Published in:
Earth Surface Processes and Landforms

DOI:
10.1002/esp.5370

Publication date:
2022

Citation for published version (APA):
Macklin, M., Booth, J., Brewer, P., Tooth, S., & Duller, G. A. T. (2022). How have Cretan rivers responded to late Holocene uplift? A multi-millennial, multi-catchment field experiment to evaluate the applicability of Schumm and Parker's (1973) complex response model. *Earth Surface Processes and Landforms*, *47*(9), 2178-2197. https://doi.org/10.1002/esp.5370

Received: 30 June 2021 | Revised: 21 March 2022 | Accepted: 24 March 2022

DOI: 10.1002/esp.5370

RESEARCH ARTICLE

ESPL WILEY

How have Cretan rivers responded to late Holocene uplift? A multi-millennial, multi-catchment field experiment to evaluate the applicability of Schumm and Parker's (1973) complex response model

Mark G. Macklin[1,2,3] | Jonathan Booth[4] | Paul A. Brewer[5] | Stephen Tooth[5] | Geoff A.T. Duller[5]

[1]The Lincoln Centre for Water and Planetary Health, and School of Geography, University of Lincoln, Lincoln, UK

[2]Innovative River Solutions, Institute of Agriculture and Environment, Massey University, Palmerston North, New Zealand

[3]Centre for the Study of the Inland, College of Arts, Social Sciences and Commerce, La Trobe University, Melbourne, Australia

[4]Vizolution, Bay Studios Business, Swansea, UK

[5]Department of Geography and Earth Sciences, Aberystwyth University, Aberystwyth, UK

Correspondence
Mark G. Macklin, The Lincoln Centre for Water and Planetary Health, and School of Geography, University of Lincoln, Brayford Pool, Lincoln LN6 7TS, UK.
Email: mmacklin@lincoln.ac.uk

Funding information
Aberystwyth University

Abstract

'Complex response' (Schumm, 1973, Geomorphic thresholds and complex response of drainage systems. In Morisawa, M. (ed.), *Fluvial Geomorphology*. Binghamton: New York State University Publications: 299-310) describes situations in which a single event triggers a series of progressively damped morphological and sedimentary adjustments within a catchment. Schumm and Parker's (1973, Implications of complex response of drainage systems for Quaternary alluvial stratigraphy. *Nature* 243: 99–100) classic stream table experiment of drainage system development showed that one baselevel fall event could result in formation of two sets of paired river terraces that need not be related to additional external (e.g., climate) influences. Despite its enduring popularity in fluvial geomorphology, large-scale and long-term field evaluations of Schumm and Parker's complex response model are very limited. Here, we report on a multi-millennial, multi-catchment field experiment in south-western Crete where a high-magnitude earthquake (estimated magnitude 8.3–8.5) on 21 July 365 CE resulted in up to 9 m of instantaneous uplift over a land area exceeding 6000 km^2. Geomorphological, sedimentological, and chronological investigations were used to investigate the erosional and depositional histories in three catchments with outlets uplifted by the 365 CE event. These catchments were compared with the Anapodaris catchment in south central Crete where baselevel was not significantly affected by the earthquake. Although all uplifted catchments experienced valley floor incision, this occurred hundreds of years after 365 CE during a period of wetter climate. The number and age of trunk stream incision and aggradation phases are similar in both uplifted and non-uplifted catchments, indicating that river responses following the 365 CE uplift event have not followed complex response trajectories in the form documented by Schumm and Parker (1973). This finding highlights the need for rigorous evaluation of other catchment or river response concepts, including through the combined use of laboratory experimental results, field data, and geochronology. In an era of rapid environmental change, characterizing and anticipating catchment and river system response increasingly will depend on a healthy interplay between different investigative approaches.

KEYWORDS
alluvial terraces, baselevel change, complex response, Holocene climate change, incision and aggradation, tectonic uplift

1 | INTRODUCTION

'Complex response' (Schumm, 1973) is a term that describes situations in which a single event and the crossing of a geomorphic threshold triggers a series of progressively damped morphological and sedimentary adjustments within a catchment. These process-form feedbacks had been demonstrated in Schumm and Parker's (1973) classic laboratory (stream table) experiment of drainage system development on a uniformly sloping, moderately cohesive (sand, silt, clay) substrate, which showed that one lowering of baselevel resulted in the formation of two sets of paired river terraces (Figure 1). The results of this laboratory experiment seemingly had profound implications for interpreting cause-and-effect relationships in fluvial sedimentary records, primarily because it suggested that not all morphological and stratigraphic discontinuities necessarily result directly from external forcing such as climate change, and that correlations of Quaternary fluvial records (e.g., terrace surfaces and alluvial fills) might be difficult (Schumm, 1973; Schumm & Parker, 1973). This was a novel and important insight, and over the half century since the publication of Schumm and Parker's (1973) paper, apparent temporal and spatial mismatches between records of fluvial erosion/deposition and external change have sometimes been attributed to variants of complex response, in whole or in part (e.g., Cheetham et al., 2010; Force, 2004; Kochel et al., 1997; Waters, 1985; Womack & Schumm, 1977). The enduring appeal of the complex response model is also demonstrated by the fact that it still commonly features as one of the first or most prominently cited examples of river response in 21st century textbooks devoted to catchment and river dynamics (e.g., Brierley & Fryirs, 2005; Fryirs & Brierley, 2013; Rhoads, 2020) and also appears in more general geomorphology and Quaternary texts (e.g., Gregory & Goudie, 2011; Gregory & Lewin, 2014; Williams, 2014).

With significant improvements since the 1970s in geochronological control provided by radiocarbon and luminescence dating, more recently researchers have demonstrated how temporal and spatial mismatches in fluvial sedimentary records in fact can be explained by reference to varying catchment and reach sensitivity to climatic drivers, governed by the interplay between sediment supply and preservation factors in alluvial record generation (Macklin & Lewin, 2008; Macklin, Lewin, et al., 2012). These factors may include, inter alia, the influence of river style, tributary-main channel coupling, valley width, and valley margin bedrock outcrop (Cohen & Nanson, 2007; Daley & Cohen, 2018; Duller et al., 2015; Keen-Zebert et al., 2013; Lewin & Macklin, 2003; Lewin et al., 2005; Tooth, 2016; Tooth et al., 2013). By contrast, a growing body of work that is based largely around generation and interpretation of laboratory experimental and computational model outputs of catchment and river development has questioned whether coherent climate signals can in fact be recorded in fluvial sediments. Instead, many studies have attributed complexity in fluvial sedimentary records to the 'shredding' of environmental signals by deterministic or stochastic, non-linear surface dynamics that collectively act as a stratigraphic filter (Jerolmack & Paola, 2010; Straub et al., 2020; Van De Wiel & Coulthard, 2010).

In any given river catchment, how do we evaluate these competing explanations for the generation of fluvial sedimentary records such as terrace sequences? For instance, do river terraces represent a complex response to baselevel fall, a response to other external drivers (e.g., climate) or other internal dynamics (e.g., non-linear sediment transport), or a response to some combination of these drivers and dynamics? With rare exceptions (e.g., Cheetham et al., 2010), to our

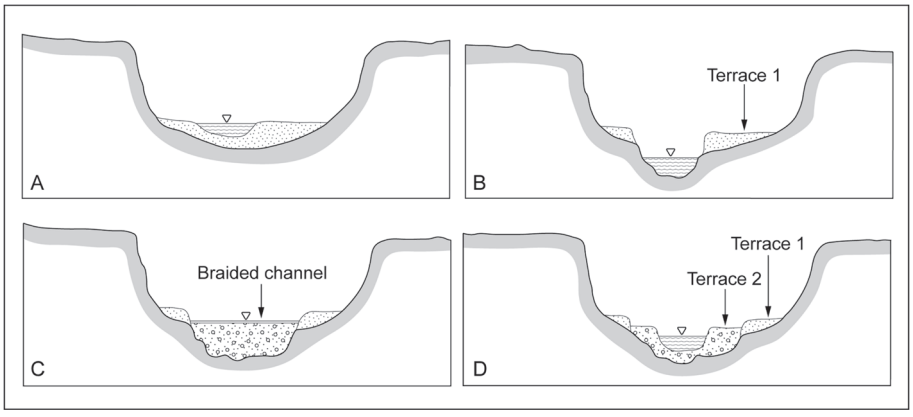

FIGURE 1 Schematic cross-sections of experimental channel 1.5 m from drainage system outlet (baselevel), showing the damped oscillatory response to 10 cm of baselevel lowering (redrawn after Schumm & Parker, 1973): (A) valley and alluvium, deposited prior to the experimental run, before baselevel lowering; (B) following baselevel lowering, channel incision forms a paired terrace and subsequent channel widening partially erodes the terrace; (C) as sediment supply from upstream initially increases, aggradation leads to development of an unstable, braided channel; (D) as sediment supply from upstream decreases, renewed incision forms a second terrace. With time, channel migration would be expected to erode part of the lower terrace and form a floodplain at a lower level

knowledge, there have been few long-term (≥ 100–1000 years) and large-scale (≥ 10–100 km^2) field evaluations of Schumm and Parker's (1973) complex response model using river terraces with secure geochronological control. More generally, given the rapid growth in laboratory experimental and computational modelling studies of fluvial system behaviour, and an associated undercurrent of scepticism from some researchers regarding the validity of invoking external (especially climate) forcing to interpret fluvial sedimentary records, there remains a need to rigorously and systematically evaluate model outputs against increasingly well-dated Pleistocene and particularly Holocene fluvial archives. Such archives are now available for many river systems worldwide (e.g., Benito, Macklin, Panin, et al., 2015; Harden et al., 2010; Macklin et al., 2006, 2015; Macklin, Fuller, et al., 2012 Panin & Matlakhova, 2015; Rădoane et al., 2019; Richardson et al., 2013).

To evaluate the applicability of Schumm and Parker's (1973) complex response model in a specific field context, and to address wider issues surrounding environmental interpretation of fluvial records, here we report the findings of a multi-millennial, multi-catchment field experiment in south-western Crete. Crete is a large (~8400 km^2) island in the Mediterranean Sea (Figure 2A), located north of the Hellenic subduction zone in one of the most seismically active regions in Europe (Pirazzoli et al., 1996; Reilinger et al., 2006). In this region, a high-magnitude earthquake (estimated minimum magnitude 8.3–8.5) on 21 July 365 CE (AD 365) caused up to ~9 m of instantaneous uplift

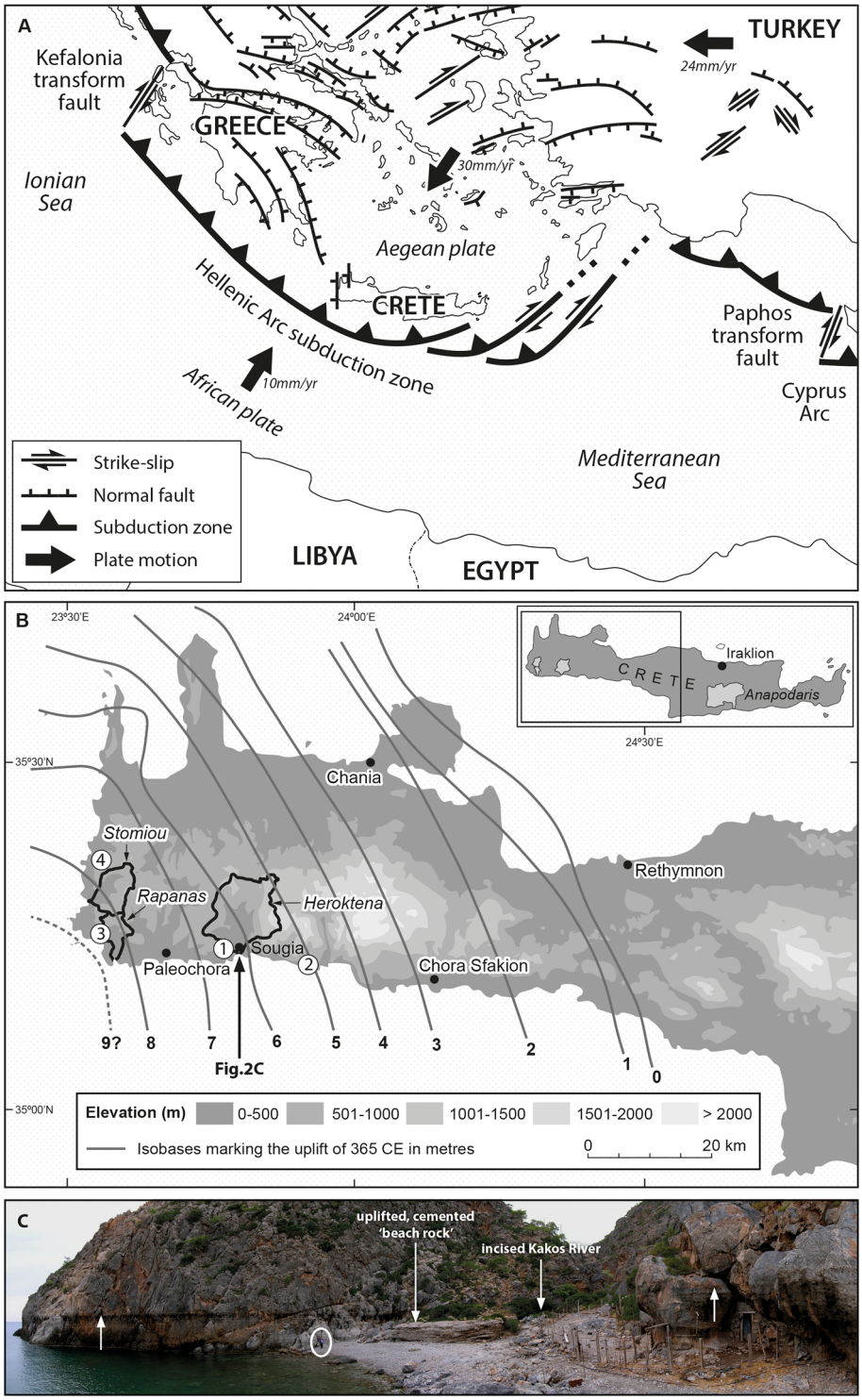

FIGURE 2 Location and characteristics of the study region. (A) Simplified map of the tectonic setting in the vicinity of Crete. The island is located to the north of the Hellenic Arc subduction zone, which is characterized by a deep (> 3000 m) trench (Hellenic Trench System) formed by descent of the African plate beneath the Aegean plate (map adapted from Taymaz et al. (2007) and Sayil (2014)). (B) Outlines of the three main study catchments in south-western Crete (Rapanas, Stomiou and Heroktena), with numbers showing locations of other catchments also investigated (1, Kakos; 2, Klados; 3, Kedrodasos; 4, Mavros). Elevation data (Copernicus, 2021) illustrate the high relative relief. Isobases show uplift in western Crete associated with the 365 CE earthquake, as reconstructed from palaeoshorelines, raised beaches, and archaeological data (adapted from Kelletat [1991] and Stiros [2010]). The location of the previously studied Anapodaris catchment (Macklin et al., 2010) is shown in the inset figure, and lies outside the uplifted area. (C) Bioerosional markers ('notches') and other features at Sougia harbour (see (B) for location) resulting from the 365 CE uplift event. The markers can be tracked along the cliff line and across the front of large boulders (see upward-pointing arrows). Uplifted, cemented 'beach rock' and the incised Kakos River provide additional evidence of landscape response to the event. A person (circled) at the foot of the cliffs provides scale. Using differential global positioning system (DGPS) measurements of the bioerosional markers and other indicators of uplift, Werner et al. (2018) established co-seismic uplift of 6.83 m at this location, confirming previous estimates of 6 to 7 m (Kelletat, 1991; Pirazzoli et al., 1982)

over a land area in western Crete exceeding 6000 km^2 (Pirazzoli et al., 1996; Shaw, 2012; Shaw et al., 2008; Stiros, 2001, 2010; Stiros & Drakos, 2006; Werner et al., 2018) (Figure 2B). Given typically steep offshore gradients (e.g., Gallen et al., 2014), regional uplift resulted in an immediate baselevel fall (relative sea level lowering) for catchments in south-western Crete, albeit to different magnitudes (Figure 2B), thereby triggering river incision in the lower reaches. The evidence of this event is recorded in the uplifted and abandoned harbour of Phalasarna on the west coast (Pirazzoli et al., 1996) and is more widely preserved around the western Crete coastline as palaeoshorelines characterized by bioerosive markers ('notches'), algal rims and raised beach deposits (e.g., Kelletat, 1991; Werner et al., 2018) (Figure 2C).

Significantly, this uplift event set in motion a possibly unique field experiment of channel and floodplain response potentially similar to that described by Schumm and Parker's (1973) laboratory experiment. In many catchments, particularly those with reaches underlain by erodible alluvial sediments, valley floor incision and aggradation phases ('cut-and-fill' cycles) in the aftermath of the uplift event have generated sets of terraces, particularly in the lowermost reaches (typically 1–2 km inland from the coastline). Hence, the aims are of this article are to: (1) use geomorphological, sedimentological, and geochronological investigations of alluvial sediments in uplifted catchments to constrain the patterns and timing of river response following the uplift event; (2) compare the pattern and timing of responses in these uplifted catchments to a previously-studied catchment in south central Crete where baselevel was not significantly affected by the earthquake (Macklin et al., 2010); (3) evaluate whether the river responses can best be interpreted as a 'classical' complex response (Schumm & Parker, 1973) to the uplift event, or as a different form of response resulting from uplift and other external (e.g., climate) and/or internal drivers and dynamics. On the basis of our findings, we then discuss the wider implications for field evaluation of river response concepts derived from laboratory experimental studies in particular, and suggest that progress in characterizing and anticipating catchment and river response increasingly will depend on a healthy interplay between different investigative approaches.

2 | REGIONAL SETTING

The island of Crete (Figure 2A) has been subject to long-term (Neogene and Quaternary), rapid uplift. Within the last 13 million years, subduction and associated co-seismic processes have resulted in cumulative net uplift of 2 to 3 km (Jolivet et al., 1996; McKenzie, 1978; Meulenkamp et al., 1994; Werner et al., 2018), with late Pleistocene rock uplift rates along the western and southern coasts estimated at up to 1.2 mm yr^{-1} (Ott et al., 2019). Consequently, Cretan catchments typically have high relative relief (Figure 2B), and tend to be characterized by high-gradient, bedrock or gravel-bed river channels that drain from mountainous headwaters (elevations widely > 1000 m and locally > 2000 m) to narrow coastal plains (Maas & Macklin, 2002; Maas et al., 1998; Macklin et al., 1995, 2010; Tooth & Nanson, 2011). River valleys are typically narrow and deep, particularly where resistant lithologies crop out. Along the south central coast alone, over 40 rivers drain predominantly limestone gorges that commonly preserve morphological and sedimentary evidence for Quaternary changes in sediment supply and flow regime that have resulted from variations in tectonic activity (including uplift, faulting, local subsidence, and seismic shaking), climate, and human land use (e.g., Booth, 2010; Bruni et al., 2021; Maas, 1998; Maas & Macklin, 2002; Maas et al., 1998; Macklin et al., 2010; Noble, 2004; Pope et al., 2008).

The area of the western Hellenic Trench System is characterized by shallow earthquakes linked to extensional faulting of the overriding plate, with deeper earthquakes being triggered by the movement of the subducted plate (Taymaz et al., 1990; Werner et al., 2018). Since the 365 CE earthquake, there have been no uplift events of this scale in western Crete (Tiberti et al., 2014), but large and often devastating earthquakes have continued to be common (Figure 3), with the impacts commonly being recorded in historical documents (AHEAD, 2021; Ambraseys, 2009; Detorakis, 1994; Noble, 2004). Many prehistoric and historical seismic events – including the 365 CE uplift event – have been associated with tsunamis that have impacted on coastal areas in Crete and the wider Mediterranean (e.g., Boulton & Whitworth, 2017; Scheffers & Scheffers, 2007; Shaw et al., 2008; Stiros, 2010; Werner et al., 2018).

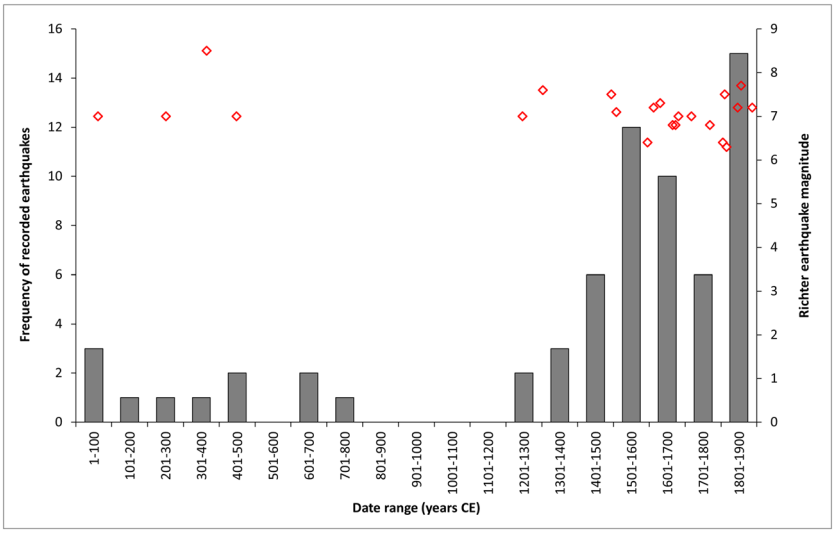

FIGURE 3 Chronology of large (> 6.0 Richter Scale) earthquakes within 50 km of the Cretan coast. Earthquake dates (grouped in 100 year bins) are from Ambraseys (2009), and magnitude data for individual events (red diamonds) are from AHEAD (2021)

Present-day climate in Crete is strongly seasonal; summers are hot and dry, and winters mild and wet. Annual precipitation totals and average temperatures are both strongly influenced by distance from the coast and by the mountainous topography. Annual precipitation ranges from 440 mm at the coast and increases inland to more than 2000 mm in some of the more mountainous regions (Koutroulis et al., 2010, 2013). In coastal locations, average monthly temperatures range from ~11°C in January to around ~27°C in July, but decrease rapidly with altitude at a rate of ~6°C per 1000 m. At altitudes above ~1000 m, much precipitation falls as snow, and winter frosts are common. Currently, the majority of Cretan rivers are ephemeral or seasonal, although a small number are supplied by natural springs and can sustain low perennial flows (Rackham & Moody, 1996). River flood events can result from snowmelt, intense localized precipitation events (> 100 mm in 24 h) and especially long duration winter storms, with more than 50% of floods occurring in November and December in association with daily precipitation maxima (Koutroulis & Tsanis, 2010; Koutroulis et al., 2010). Changes in precipitation over decadal to centennial time periods in Crete, and the frequency of floods and droughts, is controlled by latitudinal shifts in the jet stream and storm tracks (Xoplaki et al., 2004) as represented by the North Atlantic Oscillation (NAO) index. A negative NAO during the winter, associated with southward shifts of storm tracks from western Europe towards the Mediterranean, is connected with above normal precipitation over most of the Mediterranean region (Benito, Macklin, Zielhofer, et al., 2015; Maas & Macklin, 2002).

During the Holocene, human activities have impacted the Cretan landscape to varying degrees, with widespread changes to natural vegetation cover resulting from land clearance for settlements, the introduction of sheep, goats and cattle, and agricultural practices (e.g., cultivation and managed burning) (Rackham & Moody, 1996). For western Crete, regional pollen data (Jouffroy-Bapicot et al., 2016) for the last 2000 years indicate a landscape impacted by grazing and burning with three main periods: (1) evergreen oak forest (before *c.* 850 CE); 2) heather maquis (*c.* 850 to 1870 CE); (3) an open landscape with dwarf scrubs and extensive olive cultivation (*c.* 1900 CE to present). From the 20th century onwards, over-exploitation of groundwater for irrigation has also led to widespread water table declines. The impacts of these activities on hillslope sediment supply and runoff are locally significant (e.g., Jouffroy-Bapicot et al., 2016). This is especially the case in those parts of Cretan catchments underlain by more easily erodible Neogene sediments such as the Messara Plain, where major agricultural intensification led to accelerated fine-grained sedimentation in the downstream Anapodaris Gorge during the mid-12th century CE (Macklin et al., 2010). However, in the steepland catchments of south-western Crete that tend to be underlain by more mechanically resistant lithologies (e.g., limestones, phylitte quartzites), tectonic activity, climatic fluctuations, and/or stochastic events (e.g., mass movements) have been shown to be the primary controls of major valley floor incision and aggradation phases (Bruni et al., 2021; Macklin et al., 2010; Maas & Macklin, 2002; Maas et al., 1998; Pope et al., 2008, 2016). Valley-floor vegetation (e.g., maquis, phrygana, Cretan pine [*Pinus brutia*] and oleander [*Nerium oleander*]) tends to be patchy and has had little influence on these incision and aggradation phases (Maas & Macklin, 2002; Macklin et al., 2010).

3 | METHODS

To investigate the impacts of the 365 CE uplift event on river dynamics, a systematic field reconnaissance of all catchments in western Crete was undertaken, with seven chosen for more detailed geomorphological, sedimentological and geochronological investigations (Booth, 2010) (Figure 2B). These catchments were separated into those characterized in their middle-lower reaches by dominantly bedrock rivers (Kakos and Kedrodasos), dominantly alluvial rivers (Heroktena, Rapanas and Stomiou), and alluvial fans (Klados and Mavros) (Figure 2B; Table 1). In this study, we focus particular attention on the three largest catchments with their dominantly alluvial rivers (Heroktena, Rapanas and Stomiou) (Figure 2B; Table 1). To enable a direct comparison with the experiments of Schumm and Parker (1973), our detailed investigations focused on the lowermost reaches (typically 1–2 km inland from the coast, depending on catchment size and river gradient) that were directly affected by the 365 CE uplift event and where alluvial terraces are best preserved (Figure 4). The previously-studied ~500 km^2 Anapodaris catchment (Macklin et al., 2010), located ~50 km east of the area uplifted by the 365 CE event was used as a 'control' (Figure 2B; Table 1). This catchment was not significantly influenced by the uplift but has experienced similar climate and land-use histories as those catchments in western Crete affected by the earthquake (Macklin et al., 2010). The Holocene river terraces in the lowermost 4–5 km of the Anapodaris River, including those post-dating the 365 CE earthquake, have been securely dated using optically stimulated luminescence (OSL), radiocarbon, and lichenometry (Macklin et al., 2010).

3.1 | Geomorphological mapping and survey

In each of the study catchments, geomorphological features on the valley floor were mapped and topographically surveyed using a combination of differential global positioning system (DGPS) (Trimble R8 GNSS) and total station (Leica 1200) methods (horizontal accuracy ± 1.5 mm, vertical accuracy ± 3 mm). The principal geomorphological features surveyed included the channel thalweg, breaks of slope demarcating river terrace fronts, palaeochannels, alluvial fans, and the locations of OSL dating sites. These surveys were coupled with extensive sedimentological investigations, including logging of available river terrace exposures and sampling of all suitable fine-grained sediment units for subsequent OSL dating (Figure 4). In these steepland rivers, exposures of fine-grained sediment units are limited, typically being restricted to local, < 1 m thick silt and sand interbeds between coarser grained units (Figure 4). Terrace correlations were established using a combination of morphostratigraphic (using topographic data) and lithostratigraphic (sediment logs) approaches, and were subsequently field validated. All heights and upstream distances are measured from present day mean sea level as determined from the DGPS survey.

TABLE 1 Characteristics of the catchments and rivers selected for study as a part of an investigation into the geomorphic impacts of the 365 CE uplift event (after Booth, 2010). Three of these catchments (Rapanas, Stomiou and Heroktena) are the main focus of the present article. The Anapodaris catchment was studied as part of a previous investigation into river response to Holocene environmental change (Macklin et al., 2010; Noble, 2004) and is included here for comparison. Estimated 365 CE uplift values were determined from Kelletat (1991) and Stiros (2010) (cf. Figure 2B), but note that Werner et al. (2018) estimated 6.83 m of uplift at Heroktena and Kakos

	Anapodaris	Heroktena	Klados	Kakos	Kedrodasos	Mavros	Rapanas	Stomiou
Catchment area (km^2)	~500	100	12	5	2	2	20	36
Predominant geology	Limestone and flysch	Phyllite quartzites and limestone	Limestone and dolomites	Phyllite quartzites, limestone and sandstone	Phyllite quartzites	Phyllite quartzites and gypsum	Phyllite quartzites and flysch	Phyllite quartzites and gypsum
System type	Dominantly alluvial river	Dominantly alluvial river	Alluvial fan	Dominantly bedrock river	Dominantly bedrock river	Alluvial fan	Dominantly alluvial river	Dominantly alluvial river
Maximum catchment elevation (m)	1414	1984	1920	740	524	640	1010	1182
Trunk stream length (km)	37.0	15.7	6.2	4.3	2.3	3.3	9.3	9.3
Average trunk stream gradient	0.010	0.074	0.239	0.150	0.197	0.144	0.086	0.064
Estimated 365 CE uplift at catchment mouth (m)	0.0	6.3	5.0	6.3	8.8	7.7	8.5	8.5
Study reach length (m)	4800	1400	–	–	–	–	950	1650

3.2 | Optically stimulated luminescence chronology

A total of 13 samples was collected from the Rapanas, Stomiou and Heroktena catchments for OSL dating. Samples were collected using 50 mm diameter light-tight ABS Pressure Pipe Class C driven into fine-grained (silt and sand) units (typically > 30 cm thick). Samples were treated with hydrochloric acid (HCl) to remove carbonates and hydrogen peroxide (H_2O_2) to remove organic material, dry sieved to obtain grains in the range 180 to 212 μm diameter (with the exception of Irin8 and Rapa2 where grains of 150 to 212 μm were used), and density separated using sodium polytungstate at 2.62 and 2.70 g cm^{-3} to isolate the quartz fraction. The resulting material was then etched in 40% hydrofluoric acid for 40 min to remove any feldspar contamination and to remove the outer alpha-irradiated layer of the grains. The quartz grains purified by this method were measured using blue light-emitting diodes (LEDs) (470 nm) and a U-340 detection filter following a single aliquot regenerative-dose (SAR) protocol (Murray & Wintle, 2000) including a check for feldspar contamination (Duller, 2003). A dose recovery test (given dose 6.0 Gy) at preheats varying from 160 to 300°C for 10 s was undertaken on sample 129/Stom1. Aliquots were bleached by exposing them to the blue LEDs for 200 s, pausing for 10,000 s to empty the 110°C thermoluminescence (TL) peak, and then repeating the 200 s exposure to blue LEDs. Dose recovery was within 10% of unity at preheats from 180 to 300°C, but excellent precision and accuracy were seen for a preheat of 240°C (dose recovery ratio of 1.03 ± 0.03) and so this was used for all subsequent measurements.

To characterize the distribution of apparent dose, typically 30 to 47 small aliquots (covering a circle approximately 1.5 mm in diameter of the sample carrier and containing ~30 grains of the sample – Duller, 2008) were measured for each sample. The intensity of the OSL response from these aliquots was highly variable, and as has been shown previously, it is likely that the quartz OSL signal is dominated by the emission from only one or two grains. The overdispersion of the distribution was calculated, with values ranging from 7% for Aber129/Irin8 to 84% for Aber129/Irin5. Where overdispersion was 20% or lower, the Central Age Model (CAM, Galbraith et al., 1999) was used, but where overdispersion was 33% or higher the Finite Mixture Model (FMM, Galbraith & Green, 1990) was used to calculate the value of equivalent dose (D_e) used for age calculation (Figure 5; Table 2), following the approach of Rodnight et al. (2005, 2006).

Radioactivity was measured on a finely milled portion of each OSL sample, using thick-source alpha counting to determine uranium (U) and thorium (Th) concentrations and a GM25-5 beta counter (Bøtter-Jensen & Mejdahl, 1988) to determine the beta activity of the sample. By combining these two datasets, the potassium (K) concentration could be calculated (Table 2). The dose rate to the quartz grains used for luminescence measurement was calculated using beta counting data for the beta dose rate, and the U, Th and K concentrations were used to calculate the gamma dose rate. The beta and gamma dose rates were corrected for the grain size used for dating, the water content during burial, and the impact of etching with hydrofluoric acid during sample pretreatment. The cosmic dose rate was calculated based on the thickness of the overburden using the equations given in Prescott and Hutton (1994). Environmental dose

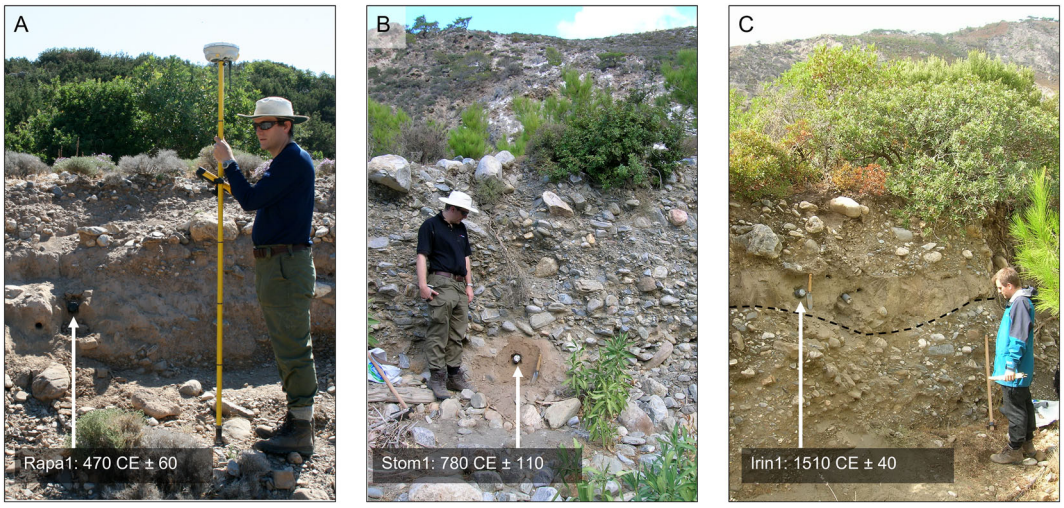

FIGURE 4 Examples of terrace sediment exposures and optically stimulated luminescence (OSL) sample sites in the three dominantly alluvial rivers: (A) Rapanas River (terrace RA1); (B) Stomiou River (terrace ST2); (C) Heroktena River (terrace HE0, with a capping flood unit [palaeochannel fill] above the dotted line). OSL ages are given in years CE; see Tables 2 and 3 for OSL analytical data, descriptions of depositional context, and corresponding ages in ka. For the location of the exposures, see the relevant sedimentological logs in Figures 6, 8 and 10

FIGURE 5 Examples of the different types of dose distributions seen in the OSL data: (A) for Rapa1, the replicate $D_e$measurements form a tight band (overdispersion 8%) and were analysed using the Central Age Model (CAM); (B) for Stom3, the $D_e$values obtained for different aliquots showed much greater scatter (overdispersion 61%) and thus the Finite Mixture Model (FMM) was used. In both cases, the grey bar shows the value determined using the model. This value is given in Table 2 and was used in age calculation

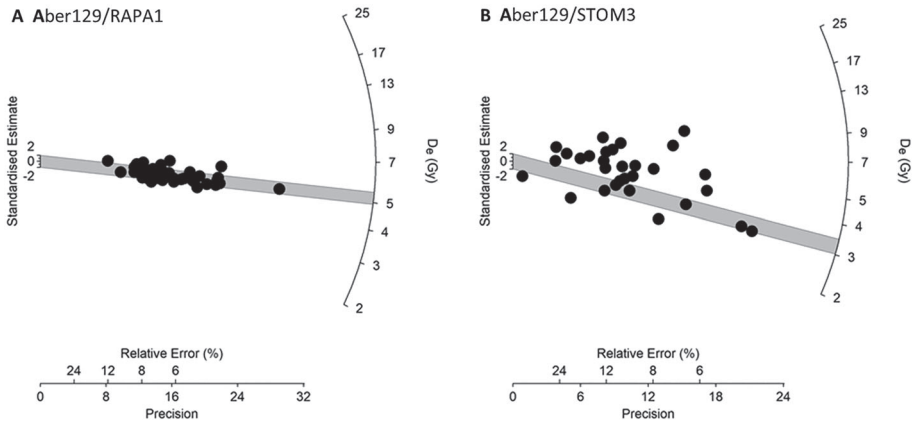

rates for the samples varied from ~2.1 to ~3.4 Gy ka^{-1} (Table 2), and the OSL ages for the samples were calculated by dividing the D_e by the dose rate (Table 2), combining errors in quadrature.

3.3 | Dendrochronology

In the Stomiou and Heroktena study reaches, additional chronological control was obtained using dendrochronology. Counting the number of annual growth rings to determine the age of a tree on an alluvial/colluvial surface is an accepted proxy for estimating the minimum age of the underlying alluvial and/or colluvial deposits (e.g., Maas, 1998). A tree borer was used to extract cores from 17 (Stomiou) and 15 (Heroktena) Cretan pine trees (*Pinus brutia*) with circumferences varying from ~10 to 280 cm that were growing on alluvial surfaces. The dark rings were counted to establish the ages of the trees, which together with the tree circumferences, were used to establish growth curves for each study reach. These curves allowed tree circumference to be used as a proxy for age, removing the need to core larger numbers of trees (Maas & Macklin, 2002).

4 | RESULTS

Geomorphological maps, sedimentological logs, and surveyed longitudinal profiles of the modern channel thalweg and terrace surfaces for the Rapanas, Stomiou and Heroktena study reaches (Figures 6–11) illustrate the spatial patterns and magnitudes of river incision and aggradation over the last few thousand years. The OSL ages (and dendrochronology ages for the Stomiou and Heroktena study reaches) indicate the timing of these changes (Figures 6–11; Tables 2 and 3). The OSL ages are consistent with the geomorphology and sedimentology; the central ages for the higher elevation terraces are older than the central ages for the lower elevation terraces, and where two ages are available in vertical sequence, then the age for the deeper sediments is older (e.g., see Figure 8, log *B*).

In the Rapanas, Stomiou and Heroktena catchments, trunk channel incision has propagated at least 700–1400 m inland since the 365 CE uplift event, and channels have extended seaward 250–300 m to below the 365 CE shoreline (Figures 6–11). Within these catchments, and in many other smaller catchments uplifted during the 365 CE earthquake (e.g., Klados, Kakos, Kedrodasos, Mavros – Table 1), the depth and inland limit of post-365 CE trunk and tributary

TABLE 2 Dose rate data, equivalent dose data and optically stimulated luminescence (OSL) ages for samples from the study catchments in south-western Crete

Terrace number	OSL sample[a]	GM25-5[b] beta dose rate (Gy ka^{-1})	U (ppm)[c]	Th (ppm)[c]	K (%)[d]	Beta[d] (Gy ka^{-1})	Gamma[e] (Gy ka^{-1})	Cosmic (Gy ka^{-1})	Total dose rate (Gy ka^{-1})	n[f]	OD (%)	Dose model[f]	D_e (Gy)	Age (ka)[g]
Rapanas														
RA1	Rapa1	2.25 ± 0.07	5.81 ± 0.41	8.28 ± 1.33	1.50 ± 0.13	1.86 ± 0.08	1.34 ± 0.09	0.19 ± 0.01	3.38 ± 0.11	47	8	CAM	5.20 ± 0.09	1.54 ± 0.06
RA2	Rapa3	1.79 ± 0.06	5.86 ± 0.32	8.78 ± 1.06	0.89 ± 0.10	1.48 ± 0.06	1.23 ± 0.07	0.17 ± 0.01	2.87 ± 0.10	43	35	FMM [30]	1.96 ± 0.15	0.68 ± 0.06
RA3	Rapa2	2.17 ± 0.07	5.11 ± 0.41	8.83 ± 1.33	1.52 ± 0.13	1.81 ± 0.08	1.29 ± 0.08	0.21 ± 0.01	3.32 ± 0.11	26	66	FMM [78]	0.65 ± 0.03	0.20 ± 0.01
Stomiou														
ST1	Stom4	1.37 ± 0.05	1.64 ± 0.34	12.52 ± 1.12	1.01 ± 0.09	1.13 ± 0.05	0.97 ± 0.07	0.18 ± 0.01	2.29 ± 0.09	30	55	FMM [16]	3.91 ± 0.38	1.71 ± 0.18
ST1	Stom6	1.68 ± 0.06	3.22 ± 0.39	12.13 ± 1.28	1.12 ± 0.11	1.39 ± 0.06	1.15 ± 0.08	0.17 ± 0.01	2.71 ± 0.10	37	47	FMM [22]	3.64 ± 0.38	1.34 ± 0.15
ST2	Stom1	1.30 ± 0.04	3.46 ± 0.28	7.42 ± 0.90	0.76 ± 0.08	1.08 ± 0.05	0.88 ± 0.06	0.16 ± 0.01	2.12 ± 0.07	28	69	FMM [36]	2.60 ± 0.22	1.23 ± 0.11
ST2	Stom3	1.80 ± 0.06	3.32 ± 0.34	11.86 ± 1.13	1.27 ± 0.11	1.49 ± 0.06	1.18 ± 0.07	0.18 ± 0.01	2.86 ± 0.10	30	61	FMM [44]	3.25 ± 0.19	1.14 ± 0.08
ST2	Stom5	1.42 ± 0.05	3.90 ± 0.27	6.49 ± 0.87	0.87 ± 0.08	1.18 ± 0.05	0.91 ± 0.06	0.22 ± 0.01	2.30 ± 0.08	34	47	FMM [41]	2.03 ± 0.17	0.88 ± 0.08
Heroktena														
HE0	Irin8	1.88 ± 0.06	4.50 ± 0.42	9.71 ± 1.37	1.23 ± 0.12	1.57 ± 0.07	1.20 ± 0.09	0.16 ± 0.01	2.93 ± 0.11	28	7	CAM	11.99 ± 0.33	4.09 ± 0.19
HE0[h]	Irin1	1.93 ± 0.06	4.02 ± 0.32	8.16 ± 1.07	1.43 ± 0.11	1.60 ± 0.07	1.13 ± 0.07	0.18 ± 0.02	2.91 ± 0.10	20	81	FMM [30]	1.44 ± 0.12	0.50 ± 0.04
HE1	Irin6	1.72 ± 0.06	3.76 ± 0.36	10.08 ± 1.18	1.15 ± 0.11	1.42 ± 0.06	1.12 ± 0.07	0.17 ± 0.01	2.71 ± 0.10	38	33	FMM [28]	5.34 ± 1.45	1.97 ± 0.54
HE2	Irin7	1.78 ± 0.06	4.16 ± 0.41	9.85 ± 1.36	1.15 ± 0.12	1.47 ± 0.06	1.15 ± 0.08	0.18 ± 0.01	2.81 ± 0.10	38	20	CAM	3.25 ± 0.11	1.16 ± 0.06
HE2[h]	Irin5	1.76 ± 0.06	4.26 ± 0.31	8.83 ± 1.01	1.15 ± 0.10	1.46 ± 0.06	1.12 ± 0.07	0.21 ± 0.01	2.79 ± 0.09	23	84	FMM [59]	0.73 ± 0.06	0.26 ± 0.02

[a]Sample name in the laboratory. The full laboratory name includes the prefix Aber129 (e.g., Aber129/Irin8).
[b]A Risø GM25-5 beta counter was used to measure the infinite matrix beta dose rate of each sample.
[c]Uranium and thorium concentrations were measured using thick-source alpha counting (TSAC), with a minimum of 3000 alpha counts for each sample.
[d]Potassium concentration was calculated using the difference between TSAC and GM25-5 beta counting.
[e]A water content of 5 ± 2% was used in dose rate calculations for all samples. Beta dose rates have been calculated to allow for the grain size analysed, the impact of hydrofluoric acid etching, and water content during burial. Gamma dose rates have been calculated to allow for water content during burial. A grain size of 180 to 212 μm was isolated for luminescence measurement for all samples except Irin8 and Rapa2 where 150–212 μm grains were used.
[f]The number of aliquots measured for each sample is given (*n*), along with the statistical dose model used to calculate the equivalent dose (D_e) used in age calculation (CAM – Central Age Model; FMM – Finite Mixture Model). For those samples analysed using the FMM, the number in the square brackets indicates the percentage of aliquots in the component used for age calculation.
[g]Age (ka) = D_e/Total Dose rate.
[h]Younger flood unit capping older terrace sediments.

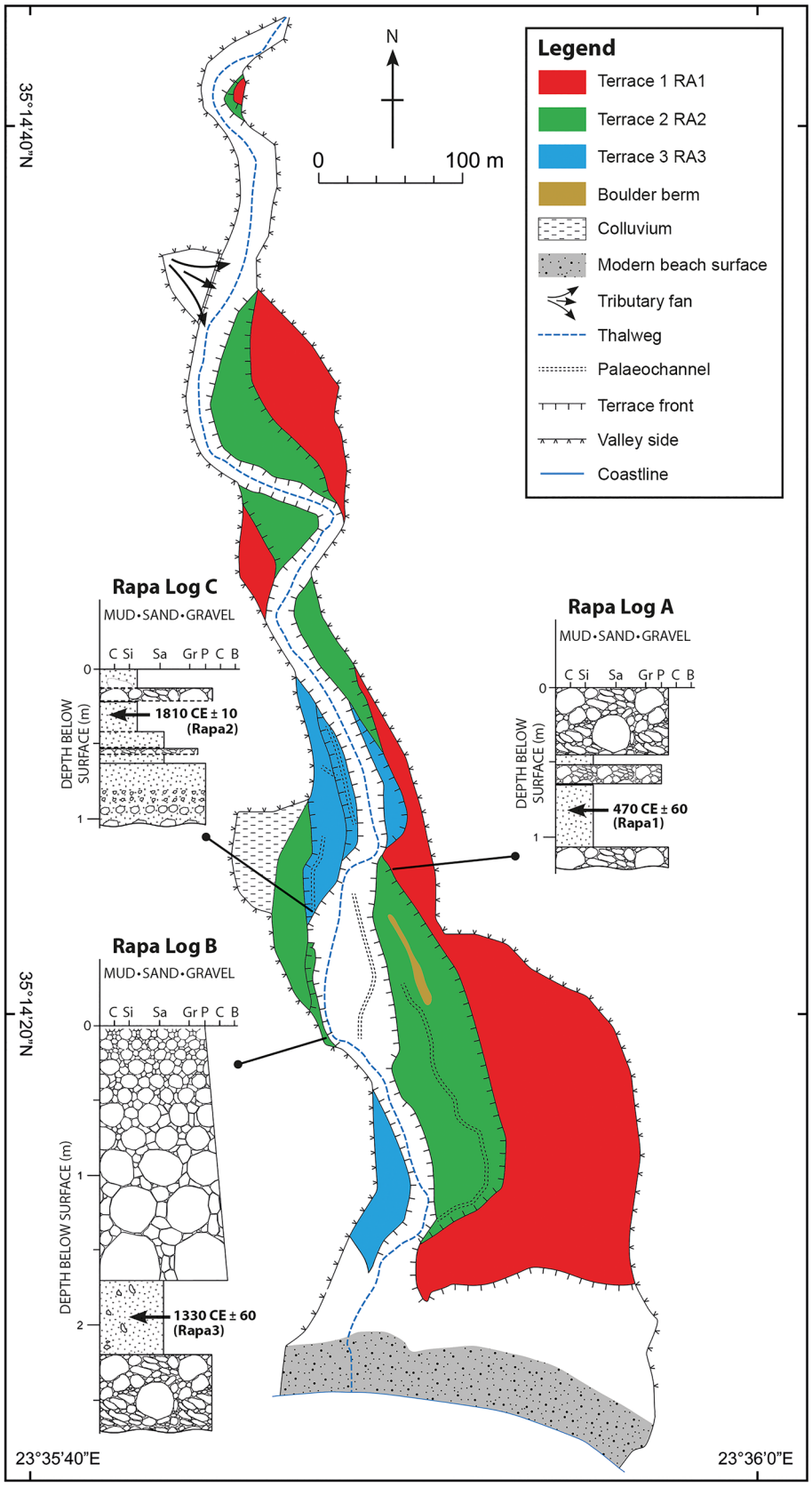

FIGURE 6 Geomorphological map of the Rapanas study reach, showing the distribution of terraces and other geomorphological features (see Figure 8 for a common sedimentological legend). Sedimentological logs show the OSL ages (in years CE) in stratigraphic context (see also Table 3)

incision is typically controlled by bedrock that crops out or lies at shallow depth (a few metres) beneath the alluvial fills (Figures 7 and 9). In the lowermost reaches of the Rapanas, Stomiou and Heroktena rivers, three paired 'cut-and-fill' terraces (cf. Macklin et al., 2013) and minor 'cut' terraces are present (Figures 6, 8 and 10) and the cumulative net depth of post-365 CE valley floor incision typically ranges from 4 to 4.6 m (Figures 7, 9 and 11).

In the lower Rapanas catchment, the longitudinal profiles of the river terraces run parallel to the contemporary river bed upstream from the 365 CE shoreline to a point ~550 m inland where they start to converge towards the channel bed (Figure 7). Downstream of the 365 CE shoreline, the terraces have higher gradients than the modern Rapanas River. In the lower Stomiou catchment, post fourth century CE terraces are generally parallel with the contemporary channel bed

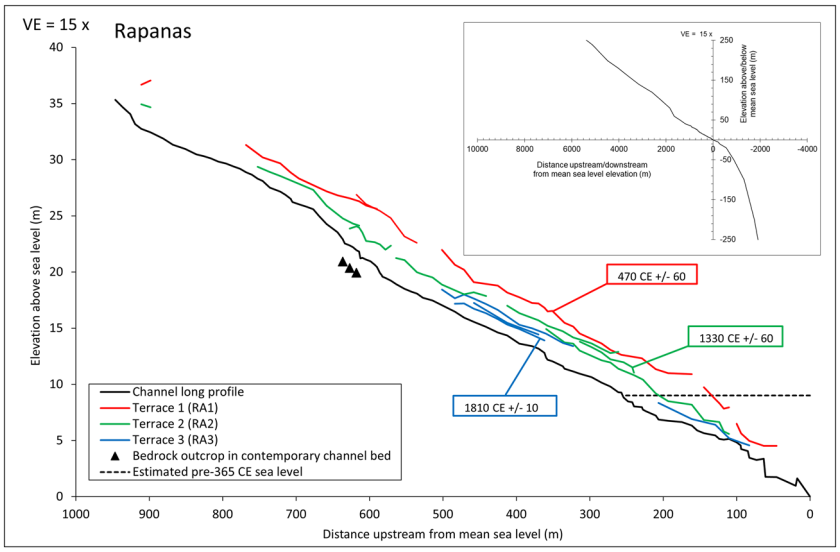

FIGURE 7 Surveyed longitudinal profiles of the modern channel thalweg and terrace surfaces for the Rapanas study reach, also indicating the associated terrace chronology in years CE (see Table 3). In some locations, access restrictions (e.g., private land) or dense vegetation prevented a full survey of each terrace front. The inset figure shows an extended long profile and illustrates the steep offshore convex gradient (based on Booth, 2010)

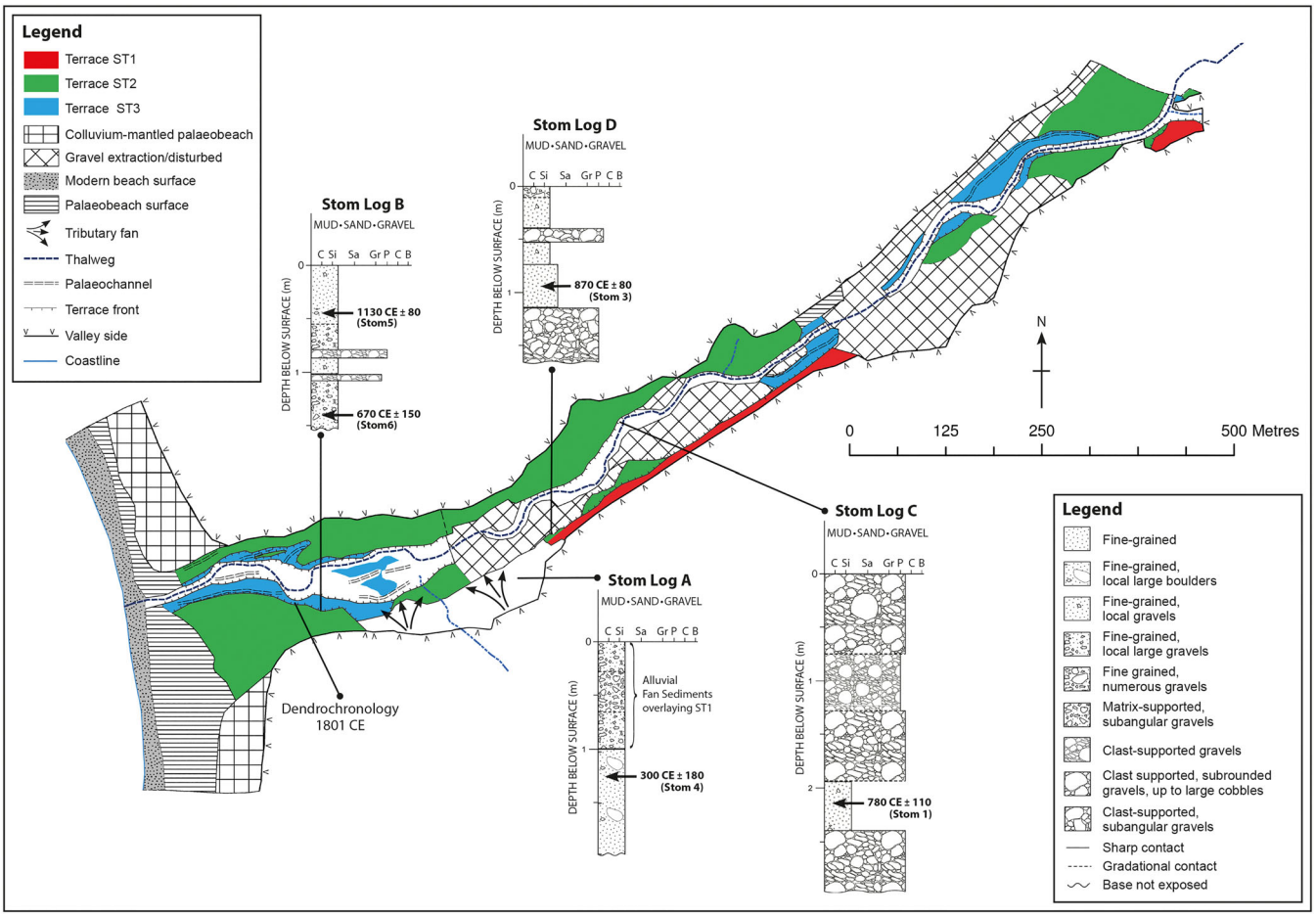

FIGURE 8 Geomorphological map of the Stomiou study reach, showing the distribution of terraces and other geomorphological features (the sedimentological legend also applies to Figures 6 and 10). Sedimentological logs show the OSL ages (in years CE) in stratigraphic context (see also Table 3)

up to *c.* 1 km inland, and then start to converge (Figure 9). Downstream of the 365 CE shoreline, terrace profiles diverge from the contemporary channel bed. In the lower Heroktena catchment, post fourth century CE and earlier Holocene terraces diverge in elevation from the contemporary channel bed upstream of the 365 CE shoreline, while downstream of this palaeoshoreline, the post fourth century CE river terraces show more of a tendency to converge towards the channel bed (Figure 11). In the lower Anapodaris catchment, which was unaffected by 365 CE uplift (Table 1), terrace profiles lie subparallel to the modern convex thalweg and there is no apparent difference in morphology between pre- and post-365 CE terraces (Macklin et al., 2010, their figure 6).

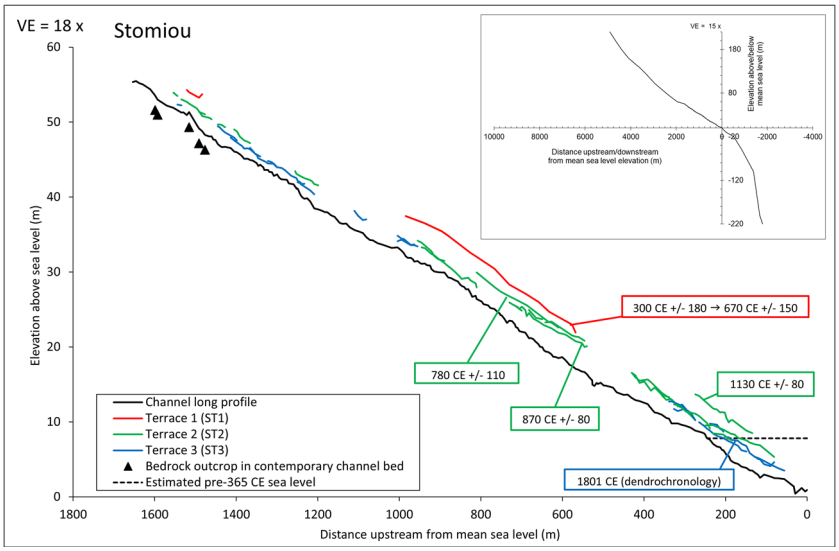

FIGURE 9 Surveyed longitudinal profiles of the modern channel thalweg and terrace surfaces for the Stomiou study reach, also indicating the associated terrace chronology in years CE (see Table 3). In some locations, access restrictions (e.g., private land) or dense vegetation prevented a full survey of each terrace front. The inset figure shows an extended long profile and illustrates the steep offshore convex gradient (based on Booth, 2010)

5 | INTERPRETATION

Since the 365 CE earthquake, no uplift events of this scale have occurred in western Crete (Tiberti et al., 2014) and across the island as a whole, large magnitude earthquakes were relatively uncommon for many hundreds of years following the uplift event (Figure 3). By contrast, various regional and local proxy records reveal marked hydroclimatic fluctuations over the same timeframe. In Figure 12, proxy records for temperature (O'Brien et al., 1995), rainfall/wet phases (Jones et al., 2006; Jouffroy-Bapicot et al., 2016), flooding (Jouffroy-Bapicot et al., 2021), and the intensity and location of the North Atlantic jet stream and storm tracks (NAO; Baker et al., 2015) are used to explore the relationship between hydroclimatic fluctuations and river dynamics, most particularly following the 365 CE earthquake. For the lower Rapanas, Stomiou and Heroktena rivers (this study), and the Anapodaris River (Macklin et al., 2010), Figure 12(F) illustrates aggradation and incision phases for the period leading up to the 365 CE earthquake and for the ~1650 years after the uplift event. The duration of aggradation phases is denoted by coloured shading and is based on OSL ages (error bar to one sigma) or dendrochronological ages for the relevant mapped river terrace (Figures 6, 8 and 10). Incision phases are identified on the basis of the mapped terrace relationships and the beginning and end of an incision phase is marked by vertical arrows with its probable time span indicated by horizontal dashed lines. OSL ages (error bar to one sigma) and dendrochronological ages from river terraces provide either a *terminus post quem* (aggradation phase preceded incision) or *terminus ante quem* (incision occurred before aggradation phase) for these incision phases.

In the centuries immediately prior to 365 CE, many rivers in south-western and south central Crete, including those whose outlets were uplifted by the earthquake (e.g., Stomiou and Heroktena) and those that lay outside of the affected area (e.g., Anapodaris), were experiencing aggradation during a multi-centennial period of warm, dry climate, and a positive phase of the NAO (Figure 12). The 365 CE tectonic event occurred during a regional drought that affected Crete and much of the eastern Mediterranean (Jones et al., 2006; Jouffroy-Bapicot et al., 2016).

These warm, dry conditions continued until *c.* 500–600 CE when there was an abrupt shift over ~50 years to a significantly wetter climate (Jouffroy-Bapicot et al., 2016) and a negative phase of the NAO that began at *c.* 600 CE and continued until *c.* 730 CE (Figure 12B–D). This shift to a wetter climate coincided with the Late Antique Little Ice Age (Büntgen et al., 2016) from 536 to 660 CE, which was marked by a notable cooling over most of the Northern Hemisphere. Well dated palaeoecological records from Asi Gonia peat bog, located at the eastern edge of the White Mountains (Lefka Ori) in western Crete, show that wetter conditions continued until *c.* 950 CE (Figure 12C; Jouffroy-Bapicot et al., 2016). A major, century-long period of flooding centred on *c.* 800 CE is also recorded at Lake Kournas, north-western Crete (Figure 12E; Jouffroy-Bapicot et al., 2021).

Following the 365 CE earthquake, incision in the Rapanas (~4.4 m), Stomiou (~4 m) and Heroktena (~4.6 m) rivers only occurred many hundreds of years later, coinciding with wetter, cooler conditions and the negative phase of the NAO. Significantly, the Anapodaris River – unaffected by the 365 CE uplift event – did not experience valley floor incision at this time. Renewed valley floor filling occurred both in the Stomiou (~3 m) and Heroktena (~2.6 m) Rivers towards the end of the eighth and beginning of the ninth centuries CE, broadly coinciding with ongoing aggradation along the Anapodaris River (Figure 12F). From the available field and geochronological evidence, no aggradation appears to have been recorded along the Rapanas River at this time (Figure 12F).

In the 14th century CE, valley floor aggradation occurred along the Rapanas (~3.3 m) and Anapodaris (~0.75 m) rivers during a wet phase (*c.* 1250–1450 CE) recorded in the Asi Gonia peat bog (Figure 12C; Jouffroy-Bapicot et al., 2016) and in the flood frequency curve at Lake Kournas (centred on *c.* 1450 CE). Aggradation was probably also occurring along the Heroktena River, but no aggradation appears to have been recorded along the Stomiou River at this time (Figure 12F).

During the 15th century CE, which coincided with the early part of the Little Ice Age, there were very significant changes in hydroclimate, with colder temperatures and a shift to a negative NAO index that persisted until the beginning of the 17th century CE (Figure 12A–D). With the possible exception of the Heroktena River, all dominantly alluvial rivers in south-western Crete uplifted by the 365 CE earthquake, and the nearby but unaffected Anapodaris River,

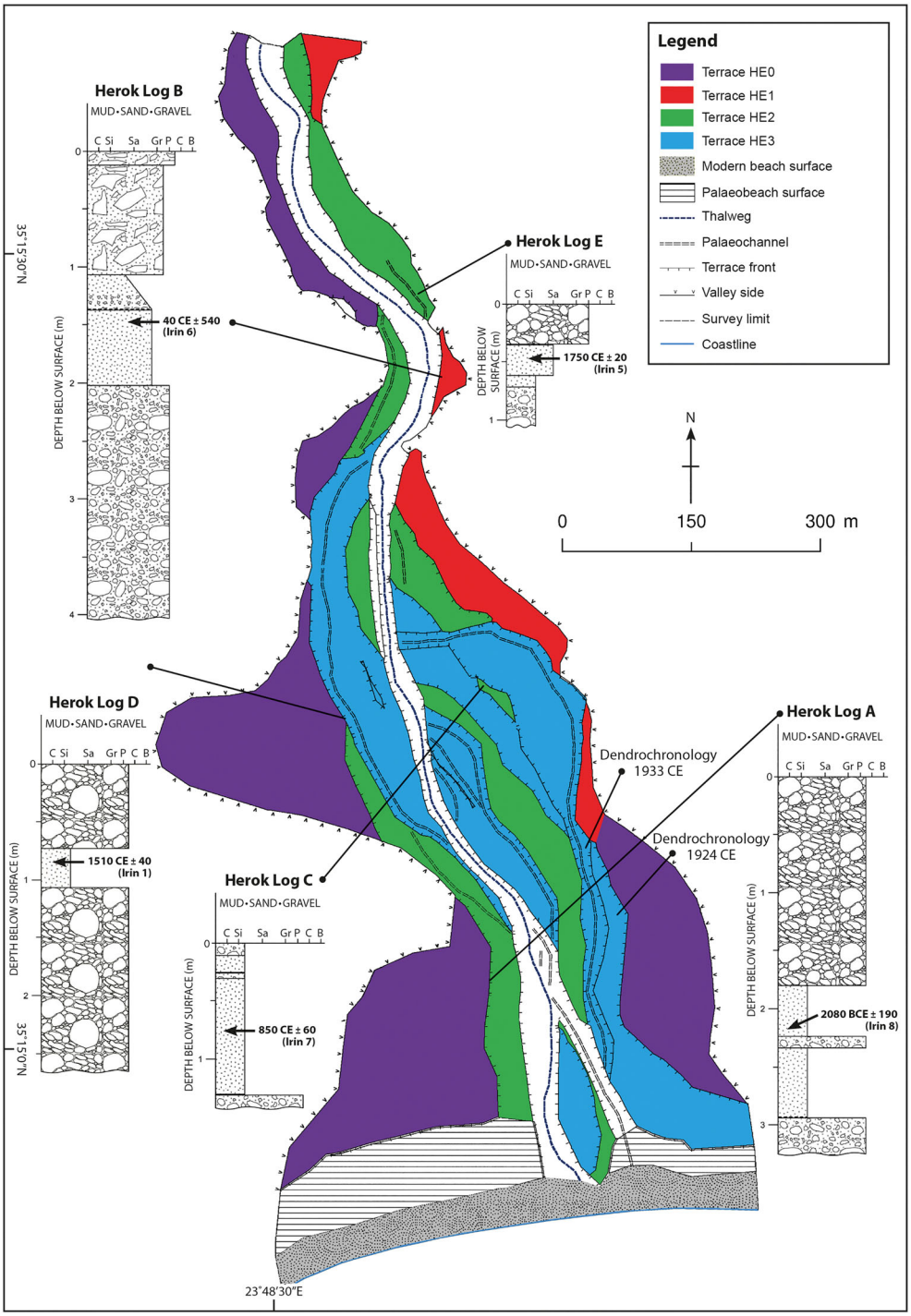

FIGURE 10 Geomorphological map of the Heroktena study reach, showing the distribution of terraces and other geomorphological features (see Figure 8 for a common sedimentological legend). Sedimentological logs show the OSL ages (in years CE) in stratigraphic context (see also Table 3)

experienced incision from 15th until the 18th centuries CE. Along the Heroktena River, evidence for incision at this time is ambiguous, with flood sedimentation on some of the higher surveyed terraces (HE0, HE2) instead providing evidence for at least localized sedimentation during individual large floods (Figures 4C, 10 and 11), before incision occurred in the mid-18th century CE (Figure 12F). Along the lower Rapanas, Stomiou and Anapodaris rivers, this incisional phase was followed by relatively minor valley floor aggradation (~2–2.2 m) during the mid to late 18th and early 19th centuries CE, coinciding with a short humid phase recorded in the Asi Gonia peat bog (*c.* 1750–1850 CE) and a predominantly negative NAO (Figure 12C-D). Along the lower Heroktena River, valley floor aggradation appears to have occurred slightly later (early 20th century CE). In the Anapodaris River, major floods in the 1840s, 1880–1890s and 1920s are recorded in the form of boulder berms and splays (Macklin et al., 2010), but the vertical tendency of all these rivers in the latter part of the record has been one of incision (Figure 12F).

The geomorphic impacts of the 365 CE earthquake on the lower reaches of dominantly alluvial rivers (Rapanas, Stomiou and Heroktena) in the uplifted region of south-western Crete can thus be

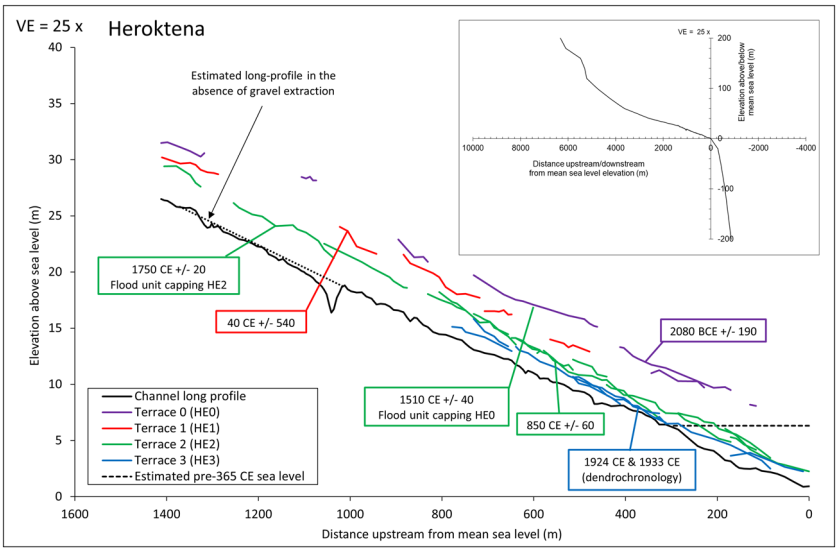

FIGURE 11 Surveyed longitudinal profiles of the modern channel thalweg and terrace surfaces for the Heroktena study reach, also indicating the associated terrace chronology in years CE (see Table 3). In some locations, access restrictions (e.g., private land) or dense vegetation prevented a full survey of each terrace front. The inset figure shows an extended long profile and illustrates the steep offshore convex gradient (based on Booth, 2010)

TABLE 3 Summary of stratigraphic context and ages for the 13 optically stimulated luminescence (OSL) samples

Terrace number	Height above thalweg (m)	Depth below surface (m)	Depositional context	Age (ka) [OSL sample]	Date (CE ± years)
Rapanas[a]					
RA1	3.6	0.9	0.4 m thick, fine-grained unit between clast-supported gravel	1.54 ± 0.06 [Rapa1]	470 ± 60
RA2	1.4	2.0	0.5 m thick, fine-grained unit between clast-supported gravel	0.68 ± 0.06 [Rapa3]	1330 ± 60
RA3	1.8	0.5	0.8 m thick, fining upwards channel fill, overlain by clast-supported gravel	0.20 ± 0.01 [Rapa2]	1810 ± 10
Stomiou[a]					
ST1	2.56	1.2	>1.0 m thick, fine-grained unit with local boulders overlain by matrix-supported, sub-angular gravel	1.71 ± 0.18 [Stom4]	300 ± 180
ST1	2.85	1.4	>0.4 m thick, fine-grained unit with local gravel	1.34 ± 0.15 [Stom6]	670 ± 150
ST2	0.23	2.2	0.5 m thick, fine-grained unit between clast-supported gravel	1.23 ± 0.11 [Stom1]	780 ± 110
ST2	1.73	1.1	0.4 m thick, fine-grained unit overlying clast-supported, sub-angular gravel	1.14 ± 0.08 [Stom3]	870 ± 80
ST2	3.79	0.5	0.6 m thick, fine-grained unit burying ST1 sediments	0.88 ± 0.08 [Stom5]	1130 ± 80
Heroktena[b]					
HE0	3.1	2.0	0.4 m thick, fine-grained unit overlain by clast-supported gravel	4.09 ± 0.19 [Irin8]	BCE 2080 ± 190
HE0[c]	5.1	1.0	0.4 m thick, fine-grained channel fill between clast-supported gravel (capping flood unit)	0.50 ± 0.04 [Irin1]	1510 ± 40
HE1	3.3	1.9	0.6 m thick, fine-grained unit overlying matrix-supported gravel	1.97 ± 0.54 [Irin6]	40 ± 540
HE2	0.6	1.1	1.0 m thick, fine-grained unit between matrix-supported gravel	1.16 ± 0.06 [Irin7]	850 ± 60
HE2[c]	3.4	0.5	0.3 m thick, fine-grained unit overlain by clast-supported gravel (capping flood unit)	0.26 ± 0.02 [Irin5]	1750 ± 20

[a]Luminescence ages given in thousands of years before measurement date of 2010 CE.
[b]Luminescence ages given in thousands of years before measurement date of 2008/2009 CE.
[c]Younger flood unit capping older terrace sediments.

summarized as: (1) deep valley floor incision extended 700–1400 m inland, but occurred hundreds of years after the 365 CE event; (2) the delay in incision coincided with an extended period of regional drought (hence, reduced river flow) that lasted until *c.* 500–600 CE, but then there was a shift to wetter conditions that ultimately led to incision; and (3) post-365 CE incision and aggradation phases have been broadly synchronous, tracked regional hydroclimatic fluctuations, and have resulted in the formation of three paired cut-and-fill terraces along each river. When compared to the timing of incision and aggradation in the nearby Anapodaris catchment unaffected by uplift, the differences in the Heroktena, Rapanas and Stomiou records suggest that river responses in these uplifted systems were strongly conditioned by the earthquake for many hundreds of years, but with the dynamics of all the rivers showing greater convergence in recent centuries.

6 | DISCUSSION

A cursory examination of river terraces in the uplifted catchments of south-western Crete, in the absence of geochronological control for the terrace sediments, might support an interpretation that river responses to the 365 CE uplift event show many morphological similarities to the complex response trajectory demonstrated in Schumm and Parker's (1973) experimental study, where sets of paired terraces formed in response to a single baselevel fall (Figure 1). Our detailed geomorphological, sedimentological and geochronological investigations, however, indicate that such an interpretation would not fully encompass the range of environmental factors that conditioned post-365 CE terrace development. The available data are sufficient to demonstrate clearly that river response to uplift (baselevel fall) has not directly followed a complex response trajectory, at least not in the form demonstrated in Schumm and Parker's (1973) study (Figure 1). Instead, uplifted dominantly alluvial rivers show a lagged incision response that reflects the effects of multi-centennial drought, followed by a direct response to short-term hydroclimatic changes (Figures 6–12) that ultimately resulted in three, rather than just two, sets of paired cut-and-fill terraces. Along these dominantly alluvial rivers, post-365 CE channel incision and its propagation inland initially took place during a period of wetter climate when flows were probably more regular and/or larger and more sediment was exported offshore. While the uplift event has an enduring legacy owing to the permanent changes to baselevel, subsequent aggradation and incision phases have coincided with short-term hydroclimatic fluctuations (Figure 12). In summary, given our extensive field data, secure geochronology, and existing independent climate proxy records, we have been able to move beyond interpretations based solely on morphostratigraphic examination of river terraces to reach a fuller, more nuanced interpretation of river response.

To our knowledge, this multi-millennial, multi-catchment evaluation of the applicability of Schumm and Parker's (1973) stream table experimental results is the first if its kind. The fact that the experimental results do not directly accord with the larger scale field reality in Crete, at least not in a straightforward manner, is perhaps unsurprising. Schumm and Parker's (1973) experiments were undertaken using a uniformly sloping (0.0075 m m^{-1}), moderately cohesive (sand, silt, clay) substrate that offered limited resistance to erosion under a steady supply of artificial rainfall and runoff. These pragmatically designed experimental boundary conditions contrast with many real-world, large-scale catchments that are characterized by different colluvial, alluvial and lithological units. By presenting varying resistance to erosion, different units influence reach-scale gradients, stream power expenditure and potential sediment supply, and thus modulate the patterns, magnitudes and rates of incisional and aggradational phases resulting from external influences. While the damped morphological response shown in Schumm and Parker's (1973) experiment might be replicated at a reach scale and over relatively short (sub-centennial) time periods in smaller, relatively homogenous catchments affected by periodic increases in sediment supply (e.g., Macklin & Lewin, 1989; Nicholas et al., 1995), in larger, more diverse catchments, greater divergence in morphological responses might be expected. Indeed, in many of our study catchments in south-western Crete, the depth and/or upstream extent of incisional phases – and hence the generation of sediment for downstream aggradational phases – commonly was limited by bedrock that cropped out on the river beds as incision proceeded (Figures 6 and 7).

In addition, within larger, more diverse catchments, the reaction and relaxation times (Graf, 1977) to a single, instantaneous baselevel change are likely to be sufficiently long (i.e., minimum of decades to millennia) that other external factors are highly unlikely to remain stationary, especially climate, as shown in our study (Figure 12). Schumm and Parker's (1973) experiment was designed in the context of trying to improve knowledge of river system response and interpretations of Quaternary fluvial sedimentary records to internal and external drivers, but what was not anticipated at the time was the subsequent revolution in palaeoclimatic research (including substantial advances in dating techniques) that increasingly have revealed evidence for high-frequency, high-magnitude palaeoclimatic fluctuations on a range of timescales, including the mid to late Holocene (e.g., Mayewski et al., 2004; Viles & Goudie, 2003). In many river catchments worldwide, including those in Crete and the wider Mediterranean (Benito, Macklin, Zielhofer, et al., 2015; Macklin et al., 2010), these palaeoclimatic fluctuations have led to profound changes in flood and drought frequency–magnitude relationships, as well as impacting directly and indirectly on sediment supply. Indeed, over the last few decades, field studies of river sensitivity and resilience to the first-order and second-order effects of these hydroclimatic fluctuations has revealed greater insights into the characteristic lags, rates and feedbacks for different river systems worldwide (e.g., Benito, Macklin, Panin, et al., 2015; Jones et al., 2015; Macklin et al., 2006; Macklin, Fuller, et al., 2012; Macklin, Lewin, et al., 2012; Toonen et al., 2017; Tooth, 2016, 2018). While there are many challenges to generating the requisite field data, especially establishing secure geochronologies for river activity and cross-correlating with independent proxy records, our study has shown that these challenges are surmountable. Building on these earlier findings, a key message from our study is that in any given catchment, the presence of multiple river terraces should not be interpreted, by default, as evidence of complex response. Complex response (Schumm & Parker, 1973) remains a possibility, but the interplay between changing baselevel, hydroclimate, and other environmental factors (e.g., land use) seems to confound the likelihood of a 'classical' complex response scenario unfolding in many larger, more diverse river catchments.

The challenges and limitations of upscaling laboratory experimental results to field reality were well appreciated by Schumm and

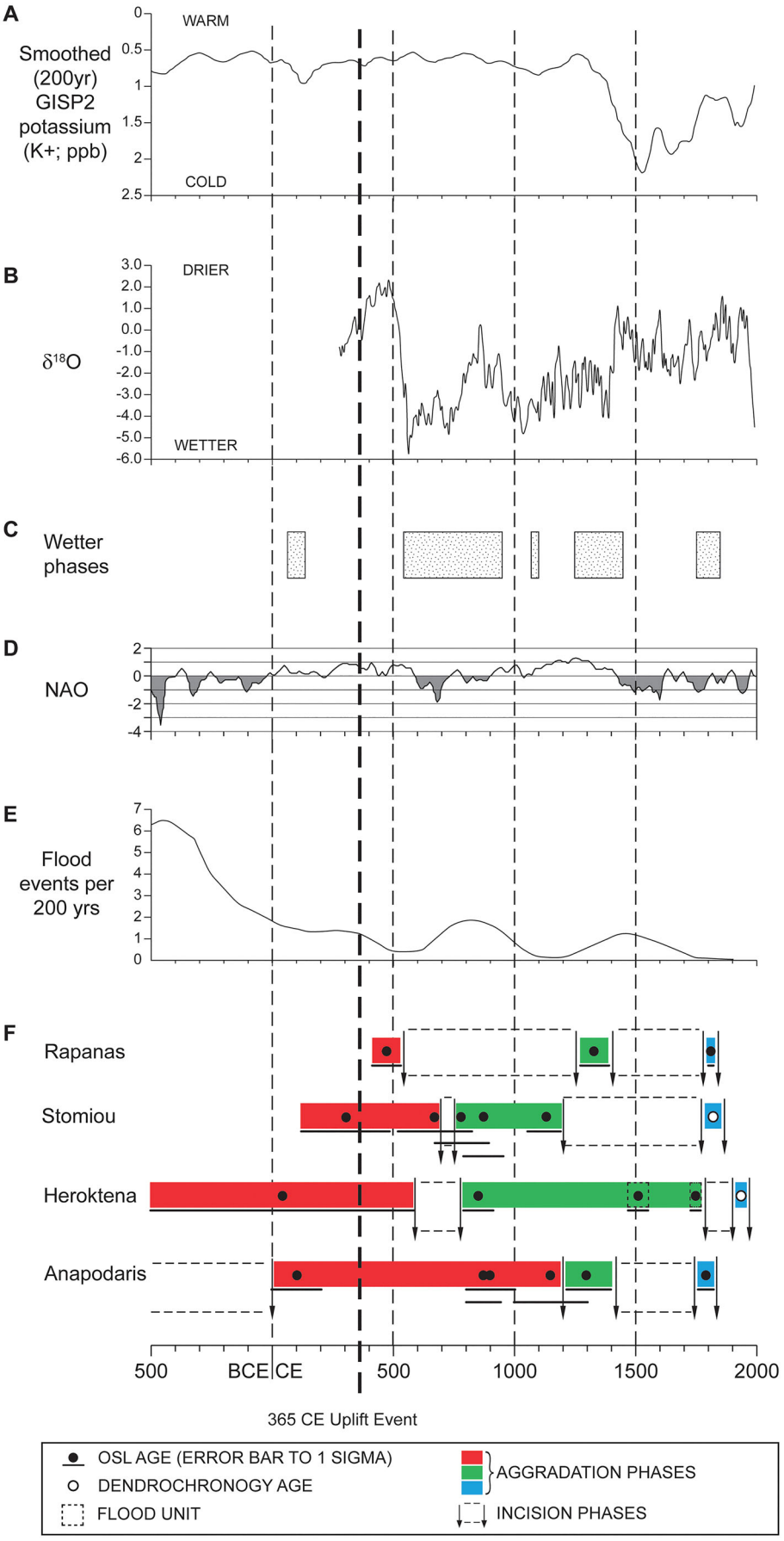

FIGURE 12 Comparison between palaeoenvironmental proxy records and river dynamics in the Rapanas, Stomiou, Heroktena and Anapodaris study reaches: (A) Gaussian smoothed (200 year) GISP2 potassium ion (K^+; ppb) proxy for the Siberian High (O'Brien et al., 1995); (B) lake oxygen isotope ($\delta^{18}O$) records from Nar Gölü (Lake Nar), Turkey, showing changes in precipitation: evaporation ratios (Jones et al., 2006; Jouffroy-Bapicot et al., 2016); (C) wetter climate phases inferred from sediment loss-on-ignition (LOI) analysis and accumulation rates for Asi Gonia peat bog, White Mountains, western Crete (Jouffroy-Bapicot et al., 2016); (D) smoothed (10 year) variability in NAO derived from a composite annual-resolution stalagmite record (Baker et al., 2015); (E) flood frequency curve for Lake Kournas, north-western Crete (Jouffroy-Bapicot et al., 2021); (F) OSL- and dendrochronology-constrained aggradation and incision phases. For clarity, the 2080 BCE ± 190 age (Irin8) for the Heroktena study reach is not shown (see Table 3), nor the older Holocene ages for samples from the Anapodaris River (see Macklin et al., 2010) but these provide maximum limiting ages for the first phase of aggradation; given the absence of older dated terrace units, similar constraints do not exist for the Rapanas and Stomiou study reaches. The duration of aggradation phases is denoted by coloured shading based on OSL ages (error bar to one sigma) or dendrochronological ages from the relevant mapped river terraces. Incision phases are marked by vertical arrows with probable time spans indicated by horizontal dashed lines. OSL ages and dendrochronological ages from river terraces provide either a *terminus post quem*(aggradation phase preceded incision) or *terminus ante quem*(incision occurred before aggradation phase) for these incision phases

colleagues (e.g., Schumm et al., 1987) but continue to provide a salutary tale. Other examples of difficulties in attempting to match laboratory experimental results with field realities can be found. For example, Holland and Pickup's (1976) classic flume study of knickpoint development in stratified sediment provided valuable insights into controls, processes and rates of 'stepped knickpoint'

retreat and associated channel adjustment but field studies in more complex sedimentological, lithological and structural terrain have indicated much greater complexity (e.g., Bishop et al., 2005; Lamb & Dietrich, 2009; Miller, 1991). From additional flume and fieldwork (e.g., Gardner, 1983), many different styles of knickpoint development are now recognized, with controls, processes and rates commonly varying widely across catchments worldwide (Goudie, 2020). Similarly, the results of laboratory 'sand box' experiments (e.g., Howard & McLane, 1988) have been widely used to provide support for the idea that groundwater sapping (seepage erosion) can lead to the development of theatre-headed valleys on Earth and other planetary bodies such as Mars (e.g., Hoke et al., 2004; Kochel et al., 1985; Laity & Malin, 1985). The role of groundwater sapping has been implicated in channel network development on a sub-kilometre or kilometre-scale in some weakly consolidated sediments (Abrams et al., 2009; Schumm et al., 1995) but application of the experimental results to explain the origin of larger, theatre-headed valleys in more resistant bedrock has been seriously questioned by subsequent fieldwork in various geological settings (e.g., Irwin et al., 2014; Lamb et al., 2006).

Collectively, these and other examples draw attention to the difficulties that are sometimes encountered in upscaling experimental model insights across space and time to account for field phenomena. Clearly, caution may need to be exercised when applying concepts derived from laboratory experiments in an attempt to try and discriminate between external (allogenic) and internal (autogenic) signals in river systems and their sedimentary records. Nevertheless, laboratory experimentation, in addition to the results derived from other investigative approaches (e.g., computational modelling) may still provide valuable insights into potential catchment and river responses, and environmental signal propagation and preservation under different combinations of topographic, geological and hydrological conditions. These insights might be very useful for exploring hypothetical scenarios of past catchment and river responses where field data has not yet been collected, or potential future response scenarios where the field evidence is yet to be generated (e.g., Lotsari et al., 2015).

7 | CONCLUSIONS

Our multi-millennial, multi-catchment field experiment in south-western Crete provides one of the first rigorous tests of the complex response trajectory shown in Schumm and Parker's (1973) classic laboratory experiment of drainage system development. Following the 365 CE uplift event, all uplifted catchments did undergo valley floor incision, but this incision only occurred hundreds of years later during a period of wetter climate, while subsequent aggradation and incision phases coincided with short-term hydroclimatic fluctuations. These findings indicate that river responses following the 365 CE event have not followed complex response trajectories in the form envisaged by Schumm and Parker (1973). Furthermore, the number and age of trunk stream incision and aggradation phases have been similar in both uplifted and non-uplifted catchments, demonstrating that inter-system correlations are possible when supported by high resolution river terrace geochronologies. This divergence from Schumm and Parker's (1973) 'classical' complex response scenario can be explained by the inclusion of additional factors in field studies, particularly when river response is occurring at a large scale in catchments with heterogeneous colluvial, alluvial and lithological substrates, and where climate is non-stationary over the relevant response and relaxation timescales.

Complex response is an enduring concept in fluvial geomorphology, and might apply in specific field settings, such as over short reaches developed in relatively homogeneous sediments. As shown by its continued inclusion in relevant textbooks (e.g., Brierley & Fryirs, 2005; Fryirs & Brierley, 2013; Gregory & Goudie, 2011; Gregory & Lewin, 2014; Rhoads, 2020; Williams, 2014), complex response also remains a concept that has great pedagogic value (e.g., for teaching about possible catchment and river response to external forcing), but its application in specific field contexts needs to be tempered by awareness of how such responses are modulated by the complexities of nature. Nearly 50 years after its initial proposal, complex response can perhaps be characterized as conceptually neat but empirically weak, as to our knowledge and prior to this study, there have been no rigorous field demonstrations in multiple river catchments of complex response in the form demonstrated by Schumm and Parker (1973). The same point could perhaps be made about some other long-cherished and newer 'complexity' concepts in fluvial geomorphology, and in geomorphology more generally (see Gregory & Lewin, 2015), particularly those concepts that cast doubt on the likelihood of preserving coherent environmental signals in fluvial sedimentary deposits. Instead, conceptual advances and pedagogic developments in (fluvial) geomorphology are more likely to result from rigorous, systematic evaluations of data derived from different investigative approaches, perhaps including comparisons between laboratory experimental results and topographically and geochronologically-constrained field data. We feel that this conclusion is one that the late Ken Gregory – armed with his acute sense of geographical differences and field realities – clearly would have recognized and appreciated.

ACKNOWLEDGEMENTS

Jonathan Booth's PhD was funded by an Aberystwyth University APRS postgraduate award. The authors thank the four anonymous reviewers and the Associate Editor for comments and suggestions that helped us to clarify our interpretations. Mark Macklin would like to dedicate this article to the late Professors Ken Gregory and Stan Schumm for sharing their wisdom and time with a young early career researcher at the University of Newcastle in the early 1980s, and for seeing the value in the convergence of contemporary and longer term studies of river landforms and sediments. Were they still to be with us today, we would love to have been able to gauge these influential individuals' responses to the article, and to have debated key points in the open-minded spirit of academic endeavour for which they were known.

AUTHOR CONTRIBUTIONS

MGM, PAB and ST conceived the project and helped to secure funding for JB's PhD studentship (which they jointly supervised). MGM, PAB and ST developed the field methodology and completed the field investigations with JB. GD undertook the luminescence dating. MGM wrote the initial draft with ST making further significant additions. PAB produced the figures and tables and drafted the methods section. MGM, PAB, ST, JB and GD were all involved in reviewing and editing the manuscript.

DATA AVAILABILITY STATEMENT

The data that support the findings of this study are available from the corresponding author, MGM, upon reasonable request.

ORCID

Mark G. Macklin https://orcid.org/0000-0003-4167-2033
Paul A. Brewer https://orcid.org/0000-0003-0834-8848
Stephen Tooth https://orcid.org/0000-0001-5714-2606
Geoff A.T. Duller https://orcid.org/0000-0002-2694-4590

REFERENCES

Abrams, D.M., Lobkovsky, A.E., Petroff, A.P., Straub, K.M., McElroy, B., Mohrig, D.C. et al. (2009) Growth laws for channel networks incised by groundwater flow. *Nature Geoscience*, 2(3), 193–196. Available from: https://doi.org/10.1038/ngeo432

AHEAD. (2021) European Archive of Historical Earthquake Data. https://www.emidius.eu/AHEAD/index.php. [4 May 2021].

Ambraseys, N. (2009) *Earthquakes in the Mediterranean and Middle East: A Multidisciplinary Study of Seismicity up to 1900*. Cambridge University Press: Cambridge. https://doi.org/10.1017/CBO9781139195430

Baker, A., Hellstrom, J.C., Kelly, B.F., Mariethoz, G. & Trouet, V. (2015) A composite annual-resolution stalagmite record of North Atlantic climate over the last three millennia. *Scientific Reports*, 5(1), 1030. Available from: https://doi.org/10.1038/srep10307

Benito, G., Macklin, M.G., Panin, A., Rossato, S., Fontana, A., Jones, A.F. et al. (2015) Recurring flood distribution patterns related to short-term Holocene climatic variability. *Scientific Reports*, 5(1), 16398. Available from: https://doi.org/10.1038/srep16398

Benito, G., Macklin, M.G., Zielhofer, C., Jones, A.F. & Machado, M.J. (2015) Holocene flooding and climate change in the Mediterranean. *Catena*, 130, 13–33. Available from: https://doi.org/10.1016/j.catena.2014.11.014

Bishop, P., Hoey, T.B., Jansen, J.D. & Artza, I.L. (2005) Knickpoint recession rate and catchment area: the case of uplifted rivers in Eastern Scotland. *Earth Surface Processes and Landforms*, 30(6), 767–778. Available from: https://doi.org/10.1002/esp.1191

Booth, J. (2010) *The response of Mediterranean steepland coastal catchments to base level and climate change, southwestern Crete*. Unpublished PhD thesis. Aberystwyth University, Aberystwyth.

Bøtter-Jensen, L. & Mejdahl, V. (1988) Assessment of beta dose-rate using a GM multicounter system. *Nuclear Tracks and Radiation Measurements*, 14(1–2), 187–191. Available from: https://doi.org/10.1016/1359-0189(88)90062-3

Boulton, S.J. & Whitworth, M.R.Z. (2017) Block and boulder accumulation on the southern coast of Crete (Greece): evidence for the 365 CE tsunami in the eastern Mediterranean. *Geological Society of London*. Special Publications, 456(1), 105–125. Available from: https://doi.org/10.1144/SP456.4

Brierley, G.J. & Fryirs, K.A. (2005) *Geomorphology and River Management: Applications of the River Styles Framework*. Blackwell Publishing: Oxford, 416 pp. https://doi.org/10.1002/9780470751367

Bruni, E.T., Ott, R.F., Picotti, V., Haghipour, N., Wegmann, K.W. & Gallen, S.F. (2021) Stochastic alluvial fan and terrace formation triggered by a high-magnitude Holocene landslide in the Klados Gorge, Crete. *Earth Surface Dynamics*, in press, 9(4), 771–793. Available from: https://doi.org/10.5194/esurf-9-771-2021

Büntgen, U., Myglan, V.S., Ljungqvist, F.C., McCormick, M., Di Cosmo, N., Sigl, M. et al. (2016) Cooling and societal change during the Late Antique Little Ice Age from 536 to around 660 AD. *Nature Geoscience*, 9(3), 231–236. Available from: https://doi.org/10.1038/ngeo2652

Cheetham, M.D., Bush, R.T., Keene, A.F. & Erskine, W.D. (2010) Non-synchronous, episodic incision: evidence of threshold exceedance and complex response as controls of terrace formation. *Geomorphology*, 123(3-4), 320–329. Available from: https://doi.org/10.1016/j.geomorph.2010.07.024

Cohen, T.J. & Nanson, G.C. (2007) Mind the gap: an absence of valley-fill deposits identifying the Holocene hypsithermal period of enhanced flow regime in southeastern Australia. *The Holocene*, 17(3), 411–418. Available from: https://doi.org/10.1177/0959683607076475

Copernicus. (2021) European Digital Elevation Model (EU-DEM), version 1.1. https://land.copernicus.eu/imagery-in-situ/eu-dem/eu-dem-v1.1?tab=mapview. [16 December 2021].

Daley, J.S. & Cohen, T.J. (2018) Climatically-controlled river terraces in eastern Australia. *Quaternary*, 1(3), 20. Available from: https://doi.org/10.3390/quat1030023

Detorakis, T.E. (1994) *History of Crete*. Geronymaki: Iraklion.

Duller, G.A.T. (2003) Distinguishing quartz and feldspar in single grain luminescence measurements. *Radiation Measurements*, 37(2), 161–165. Available from: https://doi.org/10.1016/S1350-4487(02)00170-1

Duller, G.A.T. (2008) Single grain optical dating of Quaternary sediments: why aliquot size matters in luminescence dating. *Boreas*, 37(4), 589–612. Available from: https://doi.org/10.1111/j.1502-3885.2008.00051.x

Duller, G.A.T., Tooth, S., Barham, L. & Tsukamoto, S. (2015) New investigations at Kalambo Falls, Zambia: luminescence chronology, site formation, and archaeological significance. *Journal of Human Evolution*, 85, 111–125. Available from: https://doi.org/10.1016/j.jhevol.2015.05.003

Force, E.R. (2004) Late Holocene behavior of Chaco and McElmo Canyon drainages (southwest U.S.): a comparison based on archaeologic age controls. *Geoarchaeology: An International Journal*, 19(6), 583–609. Available from: https://doi.org/10.1002/gea.20013

Fryirs, K.A. & Brierley, G.J. (2013) *Geomorphic Analysis of River Systems: An Approach to Reading the Landscape*. Wiley-Blackwell: Chichester. https://doi.org/10.1002/9781118305454

Galbraith, R.F. & Green, P.F. (1990) Estimating the component ages in a finite mixture. *Nuclear Tracks and Radiation Measurements*, 17(3), 197–206. Available from: https://doi.org/10.1016/1359-0189(90)90035-V

Galbraith, R.F., Roberts, R.G., Laslett, G.M. & Olley, J.M. (1999) Optical dating of single and multiple grains of quartz from Jinmium rock shelter, northern Australia: part 1, experimental design and statistical models. *Archaeometry*, 41(2), 339–364. Available from: https://doi.org/10.1111/j.1475-4754.1999.tb00987.x

Gallen, S.F., Wegmann, K.W., Bohnenstiehl, D.R., Pazzaglia, F.J., Brandon, M.T. & Fassoulas, C. (2014) Active simultaneous uplift and margin-normal extension in a forearc high, Crete, Greece. *Earth and Planetary Science Letters*, 398, 11–24. Available from: https://doi.org/10.1016/j.epsl.2014.04.038

Gardner, T.W. (1983) Experimental study of knickpoint and longitudinal evolution in cohesive, homogeneous material. *Geological Society of America Bulletin*, 94(5), 664–672. Available from: https://doi.org/10.1130/0016-7606(1983)94<664:ESOKAL>2.0.CO;2

Goudie, A.S. (2020) Waterfalls: forms, distribution, processes and rates of recession. *Quaestiones Geographicae*, 39(1), 59–77. Available from: https://doi.org/10.2478/quageo-2020-0005

Graf, W.L. (1977) The rate law in fluvial geomorphology. *American Journal of Science*, 277(2), 178–191. Available from: https://doi.org/10.2475/ajs.277.2.178

Gregory, K.J. & Goudie, A.S. (Eds). (2011) *The SAGE Handbook of Geomorphology*. Los Angeles: SAGE Publications.

Gregory, K.J. & Lewin, J. (2014) *The Basics of Geomorphology: Key Concepts*. SAGE Publications: Los Angeles. https://doi.org/10.4135/9781473909984

Gregory, K.J. & Lewin, J. (2015) Making concepts more explicit for geomorphology. *Progress in Physical Geography*, 39(6), 711–727. Available from: https://doi.org/10.1177/0309133315571208

Harden, T., Macklin, M.G. & Baker, V.R. (2010) Holocene flood histories in south-western USA. *Earth Surface Processes and Landforms*, 35, 707–716. Available from: https://doi.org/10.1002/esp.1983

Hoke, G.D., Isacks, B.L., Jordan, T.E. & Yu, J.S. (2004) Groundwater-sapping origin for the giant quebradas of northern Chile. *Geology*, 32(7), 605–608. Available from: https://doi.org/10.1130/G20601.1

Holland, W.N. & Pickup, G. (1976) Flume study of knickpoint development in stratified sediment. *Geological Society of America Bulletin*, 87(1), 76–82. Available from: https://doi.org/10.1130/0016-7606(1976)87<76:FSOKDI>2.0.CO;2

Howard, A.D. & McLane, C.F. (1988) Erosion of cohesionless sediment by groundwater seepage. *Water Resources Research*, 24(10), 1659–1674. Available from: https://doi.org/10.1029/WR024i010p01659

Irwin, R.P., III, Tooth, S., Craddock, R.A., Howard, A.D. & Baptista de Latour, A. (2014) Origin and development of theater-headed valleys in the Atacama Desert, northern Chile: morphological analogs to Martian valley networks. *Icarus*, 243, 296–310. Available from: https://doi.org/10.1016/j.icarus.2014.08.012

Jerolmack, D.J. & Paola, C. (2010) Shredding of environmental signals by sediment transport. *Geophysical Research Letters*, 37(19), L19401. Available from: https://doi.org/10.1029/2010GL044638

Jolivet, L., Goffé, B., Monié, P., Truffert-Luxey, C., Patriat, M. & Bonneau, M. (1996) Miocene detachment in Crete and exhumation P-T-t paths of high-pressure metamorphic rocks. *Tectonics*, 15(6), 1129e1153. Available from: https://doi.org/10.1029/96TC01417

Jones, A.F., Macklin, M.G. & Benito, G. (2015) Meta-analysis of Holocene fluvial sedimentary archives: a methodological primer. *Catena*, 130, 3–12. Available from: https://doi.org/10.1016/j.catena.2014.11.018

Jones, M.D., Roberts, C.N., Leng, M.J. & Türkeş, M. (2006) A high-resolution late Holocene lake isotope record from Turkey and links to North Atlantic and monsoon climate. *Geology*, 34(5), 361–364. Available from: https://doi.org/10.1130/G22407.1

Jouffroy-Bapicot, I., Pedrotta, T., Debret, M., Field, S., Sulpizio, R., Zanchetta, G. et al. (2021) Olive groves around the lake. A ten-thousand-year history of a Cretan landscape (Greece) reveals the dominant role of humans in making this Mediterranean ecosystem. *Quaternary Science Reviews*, 267, 107072. Available from: https://doi.org/10.1016/j.quascirev.2021.107072

Jouffroy-Bapicot, I., Vannière, B., Iglesias, V., Debret, M. & Delarras, J.-F. (2016) 2000 years of grazing history and the making of the Cretan mountain landscape, Greece. *PLoS ONE*, 11(6), e0156875. Available from: https://doi.org/10.1371/journal.pone.0156875

Keen-Zebert, A., Tooth, S., Rodnight, H., Duller, G.A.T., Roberts, H.M. & Grenfell, M. (2013) Late Quaternary floodplain reworking and the preservation of alluvial sedimentary archives in unconfined and confined river valleys in the eastern interior of South Africa. *Geomorphology*, 185, 54–66. Available from: https://doi.org/10.1016/j.geomorph.2012.12.004

Kelletat, D. (1991) The 1550 BP tectonic event in the eastern Mediterranean as a basis for assuring the intensity of shore processes. *Zeitschrift für Geomorphologie*, 81, 181–194.

Kochel, R.C., Howard, A.D. & McLane, C.F. (1985) Channel networks developed by groundwater sapping in fine-grained sediments: analogs to some Martian valleys. In: Woldenberg, M. (Ed.) *Models in Geomorphology*. St. Leonards, N.S.W., Australia: Allen and Unwin, pp. 313–341.

Kochel, R.C., Miller, J.R. & Ritter, D.F. (1997) Geomorphic response to minor cyclic climate changes, San Diego County, California. *Geomorphology*, 19(3–4), 277–302. Available from: https://doi.org/10.1016/S0169-555X(97)00013-5

Koutroulis, A.G. & Tsanis, I.K. (2010) A method for estimating flash flood peak discharge in a poorly gauged basin: case study for the 13-14 January 1994 flood, Giofiros basin, Crete, Greece. *Journal of Hydrology*, 385(1–4), 150–164. Available from: https://doi.org/10.1016/j.jhydrol.2010.02.012

Koutroulis, A.G., Tsanis, I.K. & Daliakopoulos, I.N. (2010) Seasonality of floods and their hydrometeorologic characteristics in the island of Crete. *Journal of Hydrology*, 394(1–2), 90–100. Available from: https://doi.org/10.1016/j.jhydrol.2010.04.025

Koutroulis, A.G., Tsanis, I.K., Daliakopoulos, I.N. & Jacob, D. (2013) Impact of climate change on water resources status: a case study for Crete Island, Greece. *Journal of Hydrology*, 479, 146–158. Available from: https://doi.org/10.1016/j.jhydrol.2012.11.055

Laity, J.E. & Malin, M.C. (1985) Sapping processes and the development of theater-headed valley networks on the Colorado Plateau. *Geological Society of America Bulletin*, 96(2), 203–217. Available from: https://doi.org/10.1130/0016-7606(1985)96<203:SPATDO>2.0.CO;2

Lamb, M.P. & Dietrich, W.E. (2009) The persistence of waterfalls in fractured rock. *Geological Society of America Bulletin*, 121(7–8), 1123–1134. Available from: https://doi.org/10.1130/B26482.1

Lamb, M.P., Howard, A.D., Johnson, J., Whipple, K.X., Dietrich, W.E. & Perron, J.T. (2006) Can springs cut canyons into rock? *Journal of Geophysical Research: Planets*, 111(E7), E07002. Available from: https://doi.org/10.1029/2005JE002663

Lewin, J. & Macklin, M.G. (2003) Preservation potential for Late Quaternary river alluvium. *Journal of Quaternary Science*, 18(2), 107–120. Available from: https://doi.org/10.1002/jqs.738

Lewin, J., Macklin, M.G. & Johnstone, E. (2005) Interpreting alluvial archives: sedimentological factors in the British Holocene fluvial record. *Quaternary Science Reviews*, 24(16–17), 1873–1889. Available from: https://doi.org/10.1016/j.quascirev.2005.01.009

Lotsari, E., Thorndycraft, V. & Alho, P. (2015) Prospects and challenges of simulating river channel response to future climate change. *Progress in Physical Geography*, 39(4), 483–513. Available from: https://doi.org/10.1177/0309133315578944

Maas, G.S. (1998) *River response to Quaternary environmental change, southwestern Crete. Greece. Greece*. Unpublished PhD thesis. University of Leeds.

Maas, G.S. & Macklin, M.G. (2002) The impact of recent climate change on flooding and sediment supply within a Mediterranean mountain catchment, southwestern Crete, Greece. *Earth Surface Processes and Landforms*, 27(10), 1087–1105. Available from: https://doi.org/10.1002/esp.398

Maas, G.S., Macklin, M.G. & Kirkby, M.J. (1998) Late Pleistocene and Holocene river development in Mediterranean steepland environments, southwest Crete, Greece. In: Benito, G., Baker, V.R. & Gregory, K.J. (Eds.) *Palaeohydrology and Environmental Change*. Chichester: John Wiley and Sons, pp. 153–165.

Macklin, M.G., Benito, G., Gregory, K.J., Johnstone, E., Lewin, J., Michczyńska, D.J., Soja, R., Starkel, L. & Thorndycraft, V.R. (2006) Past hydrological events reflected in the Holocene fluvial record of Europe. *Catena*, 66(1–2), 145–154. Available from: https://doi.org/10.1016/j.catena.2005.07.015

Macklin, M.G., Fuller, I.C., Jones, A.F. & Bebbington, M. (2012) New Zealand and UK Holocene flooding demonstrates interhemispheric climate asynchrony. *Geology*, 40(9), 775–778. Available from: https://doi.org/10.1130/G33364.1

Macklin, M.G. & Lewin, J. (1989) Sediment transfer and transformation of an alluvial valley floor: the River South Tyne, Northumbria, UK. *Earth Surface Processes and Landforms*, 14(3), 233–246. Available from: https://doi.org/10.1002/esp.3290140305

Macklin, M.G. & Lewin, J. (2008) Alluvial responses to the changing Earth system. *Earth Surface Processes and Landforms*, 33(9), 1374–1395. Available from: https://doi.org/10.1002/esp.1714

Macklin, M.G., Lewin, J. & Jones, A.F. (2013) River entrenchment and terrace formation in the UK Holocene. *Quaternary Science Reviews*, 76, 194–206. Available from: https://doi.org/10.1016/j.quascirev.2013.05.026

Macklin, M.G., Lewin, J. & Woodward, J.C. (1995) Quaternary fluvial systems in the Mediterranean basin. In: Woodward, J.C., Lewin, J. & Macklin, M.G. (Eds.) *Mediterranean Quaternary River Environments*. AA Balkema, Rotterdam, pp. 1–25.

Macklin, M.G., Lewin, J. & Woodward, J.C. (2012) The fluvial record of climate change. *Philosophical Transactions of the Royal Society a: Mathematical, Physical and Engineering Sciences*, 370(1966), 2143–2172. Available from: https://doi.org/10.1098/rsta.2011.0608

Macklin, M.G., Toonen, W.H., Woodward, J.C., Williams, M.A., Flaux, C., Marriner, N., Nicoll, K., Verstraeten, G., Spencer, N. & Welsby, D. (2015) A new model of river dynamics, hydroclimatic change and human settlement in the Nile Valley derived from meta-analysis of the Holocene fluvial archive. *Quaternary Science Reviews*, 130, 109–123. Available from: https://doi.org/10.1016/j.quascirev.2015.09.024

Macklin, M.G., Tooth, S., Brewer, P.A., Noble, P.L. & Duller, G.A.T. (2010) Holocene flooding and river development in a Mediterranean steepland catchment: the Anapodaris Gorge, south central Crete, Greece. *Global and Planetary Change*, 70(1–4), 35–52. Available from: https://doi.org/10.1016/j.gloplacha.2009.11.006

Mayewski, P.A., Rohling, E.E., Stager, J.C., Karlén, W., Maasch, K.A., Meeker, L.D. et al. (2004) Holocene climate variability. *Quaternary Research*, 62(3), 243–255. Available from: https://doi.org/10.1016/j.yqres.2004.07.001

McKenzie, D. (1978) Active tectonics of the alpine Himalayan belt, the Aegean Sea and surrounding regions. *Geophysical Journal International*, 55(1), 217–254. Available from: https://doi.org/10.1111/j.1365-246X.1978.tb04759.x

Meulenkamp, J.E., van der Zwaan, G.J. & van Wamel, W.A. (1994) On late Miocene to recent vertical motions in the Cretan segment of the Hellenic arc. *Tectonophysics*, 234(1–2), 53–72. Available from: https://doi.org/10.1016/0040-1951(94)90204-6

Miller, J.R. (1991) The influence of bedrock geology on knickpoint development and channel-bed degradation along downcutting streams in south-central Indiana. *Journal of Geology*, 99(4), 591–605. Available from: https://doi.org/10.1086/629519

Murray, A.S. & Wintle, A.G. (2000) Luminescence dating of quartz using an improved single-aliquot regenerative-dose protocol. *Radiation Measurements*, 32(1), 57–73. Available from: https://doi.org/10.1016/S1350-4487(99)00253-X

Nicholas, A.P., Ashworth, p.J., Kirkby, M.J., Macklin, M.G. & Murray, T. (1995) Sediment slugs: large-scale fluctuations in fluvial sediment transport rates and storage volumes. *Progress in Physical Geography*, 19(4), 500–519. Available from: https://doi.org/10.1177/030913339501900404

Noble, P.L. (2004) *Response of a steepland river system to late Quaternary environmental change: south central Crete*. Unpublished PhD thesis. University of Wales, Aberystwyth.

O'Brien, S.R., Mayewski, P.A., Meeker, L.D., Meese, D.A., Twickler, M.S. & Whitlow, S.I. (1995) Complexity of Holocene climate as reconstructed from a Greenland ice core. *Science*, 270(5244), 1962–1964. Available from: https://doi.org/10.1126/science.270.5244.1962

Ott, R.F., Gallen, S.F., Wegmann, K.W., Biswas, R.H., Herman, F. & Willett, S.D. (2019) Pleistocene terrace formation, Quaternary rock uplift rates and geodynamics of the Hellenic Subduction Zone revealed from dating of paleoshorelines on Crete, Greece. *Earth and Planetary Science Letters*, 525, 115757. Available from: https://doi.org/10.1016/j.epsl.2019.115757

Panin, A. & Matlakhova, E. (2015) Fluvial chronology in the East European Plain over the last 20 ka and its palaeohydrological implications. *Catena*, 130, 46–61. Available from: https://doi.org/10.1016/j.catena.2014.08.016

Pirazzoli, P., Laborel, J. & Stiros, S.C. (1996) Earthquake clustering in the Eastern Mediterranean during historical times. *Journal of Geophysical Research: Solid Earth*, 101(B3), 6083–6097. Available from: https://doi.org/10.1029/95JB00914

Pirazzoli, P.A., Thommeret, J., Thommeret, Y., Laborel, J. & Montaggioni, L.F. (1982) Crustal block-movements from Holocene shorelines: Crete and Antikythira (Greece). *Tectonophysics*, 86(1–3), 27–43. Available from: https://doi.org/10.1016/0040-1951(82)90060-9

Pope, R., Wilkinson, K., Skourtsos, E., Triantaphyllou, M. & Ferrier, G. (2008) Clarifying stages of alluvial fan evolution along the Sfakian piedmont, southern Crete: new evidence from analysis of post-incisive soils and OSL dating. *Geomorphology*, 94(1-2), 206–225. Available from: https://doi.org/10.1016/j.geomorph.2007.05.007

Pope, R.J., Candy, I. & Skourtsos, E. (2016) A chronology of alluvial fan response to Late Quaternary sea level and climate change, Crete. *Quaternary Research*, 86(2), 170–183. Available from: https://doi.org/10.1016/j.yqres.2016.06.003

Prescott, J.R. & Hutton, J.T. (1994) Cosmic ray contributions to dose rates for luminescence and ESR dating: large depths and long-term time variations. *Radiation Measurements*, 23(2–3), 497–500. Available from: https://doi.org/10.1016/1350-4487(94)90086-8

Rackham, O. & Moody, J. (1996) *The Making of the Cretan Landscape*. Manchester: Manchester University Press.

Rădoane, M., Chiriloaei, F., Sava, T., Nechita, C., Rădoane, N. & Gâza, O. (2019) Holocene fluvial history of Romanian Carpathian rivers. *Quaternary International*, 527, 113–129. Available from: https://doi.org/10.1016/j.quaint.2018.11.014

Reilinger, R., McClusky, S., Vernant, P., Lawrence, S., Ergintav, S., Cakmak, R. et al. (2006) GPS constraints on continental deformation in the Africa-Arabia-Eurasia continental collisional zone and implications for the dynamics of plate interactions. *Journal of Geophysical Research: Solid Earth*, 111(B5), B05411. Available from: https://doi.org/10.1029/2005JB004051

Rhoads, B.L. (2020) *River Dynamics: Geomorphology to Support Management*. Cambridge University Press: New York, https://doi.org/10.1017/9781108164108

Richardson, J.M., Fuller, I.C., Macklin, M.G., Jones, A.F., Holt, K.A., Litchfield, N.J. & Bebbington, M. (2013) Holocene river behaviour in New Zealand: response to regional centennial-scale climate forcing. *Quaternary Science Reviews*, 69, 8–27. Available from: https://doi.org/10.1016/j.quascirev.2013.02.021

Rodnight, H., Duller, G.A.T., Tooth, S. & Wintle, A.G. (2005) Optical dating of a scroll-bar sequence on the Klip River, South Africa, to derive the lateral migration rate of a meander bend. *The Holocene*, 15(6), 802–811. Available from: https://doi.org/10.1191/0959683605hl854ra

Rodnight, H., Duller, G.A.T., Wintle, A.G. & Tooth, S. (2006) Assessing the reproducibility and accuracy of optical dating of fluvial deposits. *Quaternary Geochronology*, 1(2), 109–120. Available from: https://doi.org/10.1016/j.quageo.2006.05.017

Sayil, N. (2014) Evaluation of the seismicity for the Marmara region with statistical approaches. *Acta Geodaetica et Geophysica Hungarica*, 49(3), 265–281. Available from: https://doi.org/10.1007/s40328-014-0058-4

Scheffers, A. & Scheffers, S. (2007) Tsunami deposits on the coastline of west Crete (Greece). *Earth and Planetary Science Letters*, 259(3-4), 613–624. Available from: https://doi.org/10.1016/j.epsl.2007.05.041

Schumm, S.A. (1973) Geomorphic thresholds and complex response of drainage systems. In: Morisawa, M. (Ed.) *Fluvial Geomorphology*, Vol. 3. Publications in Geomorphology, State University of New York, Binghamton, pp. 299–310.

Schumm, S.A., Boyd, K.F., Wolff, C.G. & Spitz, W.J. (1995) A groundwater sapping landscape in the Florida Panhandle. *Geomorphology*, 12(4), 281–297. Available from: https://doi.org/10.1016/0169-555X(95)00011-S

Schumm, S.A., Mosley, M.P. & Weaver, W.E. (1987) *Experimental Fluvial Geomorphology*. New York: John Wiley and Sons.

Schumm, S.A. & Parker, R.S. (1973) Implications of complex response of drainage systems for Quaternary alluvial stratigraphy. *Nature*, 243(128), 99–100. Available from: https://doi.org/10.1038/physci243099a0

Shaw, B. (2012) *Active Tectonics of the Hellenic Subduction Zone*. Springer Theses: Heidelberg, https://doi.org/10.1007/978-3-642-20804-1

Shaw, B., Ambraseys, N.N., England, P.C., Floyd, M.A., Gorman, G.J., Higham, T.F.G. et al. (2008) Eastern Mediterranean tectonics and tsunami hazard inferred from the AD 365 earthquake. *Nature Geoscience*, 1(4), 268–276. Available from: https://doi.org/10.1038/ngeo151

Stiros, S. (2001) The AD 365 Crete earthquake and possible seismic clustering during the fourth to sixth centuries AD in the Eastern Mediterranean: a review of historical and archaeological data. *Journal of Structural Geology*, 23(2–3), 545–562. Available from: https://doi.org/10.1016/S0191-8141(00)00118-8

Stiros, S.C. (2010) The 8.5+ magnitude, AD365 earthquake in Crete: coastal uplift, topography changes, archaeological and historical signature. *Quaternary International*, 216(1–2), 54–63. Available from: https://doi.org/10.1016/j.quaint.2009.05.005

Stiros, S.C. & Drakos, A. (2006) A fault-model for the tsunami-associated, magnitude ≥ 8.5 Eastern Mediterranean, AD365 earthquake. *Zeitschrift für Geomorphologie, Supplement*, 146, 139–172.

Straub, K.M., Duller, R.A., Foreman, B.Z. & Hajek, E.A. (2020) Buffered, incomplete, and shredded: the challenges of reading an imperfect stratigraphic record. *Journal of Geophysical Research: Earth Surface*, 125, 2019JF005079.

Taymaz, T., Jackson, J. & Westaway, R. (1990) Earthquake mechanisms in the Hellenic Trench near Crete. *Geophysical Journal International*, 102(3), 695–731. Available from: https://doi.org/10.1111/j.1365-246X.1990.tb04590.x

Taymaz, T., Yilmaz, Y. & Dilek, Y. (2007) The geodynamics of the Aegean and Anatolia: introduction. In Taymaz, T., Yilmaz, Y. & Dilek, Y. (Eds) *The Geodynamics of the Aegean and Anatolia*. Geological Society, London, Special Publications, London, 291(1), 1–16. https://doi.org/10.1144/SP291.1

Tiberti, M., Basili, R. & Vannoli, P. (2014) Ups and downs in western Crete (Hellenic subduction zone). *Scientific Reports*, 4, 5677. https://doi.org/10.1038/srep05677

Toonen, W.H., Foulds, S.A., Macklin, M.G. & Lewin, J. (2017) Events, episodes, and phases: signal from noise in flood-sediment archives. *Geology*, 45(4), 331–334. Available from: https://doi.org/10.1130/G38540.1

Tooth, S. (2016) Changes in fluvial systems during the Quaternary. In: Knight, J. & Grab, S. (Eds.) *Quaternary Environmental Change in Southern Africa: Physical and Human Dimensions*. Cambridge: Cambridge University Press, pp. 170–187.

Tooth, S. (2018) The geomorphology of wetlands in drylands: resilience, nonresilience, or … ?, Proceedings of the 2017 Binghamton Symposium in Geomorphology. *Geomorphology*, 305, 33–48. Available from: https://doi.org/10.1016/j.geomorph.2017.10.017

Tooth, S., Hancox, P.J., Brandt, D., McCarthy, T.S., Jacobs, Z. & Woodborne, S.M. (2013) Controls on the genesis, sedimentary architecture, and preservation potential of dryland alluvial successions in stable continental interiors: insights from the incising Modder River, South Africa. *Journal of Sedimentary Research*, 83(7), 541–561. Available from: https://doi.org/10.2110/jsr.2013.46

Tooth, S. & Nanson, G.C. (2011) Distinctiveness and diversity of arid zone rivers. In Thomas, D.S.G. (Ed.) *Arid Zone Geomorphology: Process, Form and Change in Drylands (3rd Edition)*. Wiley: Chichester; 269–300, https://doi.org/10.1002/9780470710777.ch12

Van De Wiel, M.J. & Coulthard, T.J. (2010) Self-organized criticality in river basins: challenging sedimentary records of environmental change. *Geology*, 38(1), 87–90. Available from: https://doi.org/10.1130/G30490.1

Viles, H.A. & Goudie, A.S. (2003) Interannual, decadal and multidecadal scale climatic variability and geomorphology. *Earth-Science Reviews*, 61(1–2), 105–131. Available from: https://doi.org/10.1016/S0012-8252(02)00113-7

Waters, M.R. (1985) Late Quaternary alluvial stratigraphy of Whitewater Draw, Arizona: implications for regional correlation of fluvial deposits in the American Southwest. *Geology*, 13(10), 705–708. Available from: https://doi.org/10.1130/0091-7613(1985)13<705:LQASOW>2.0.CO;2

Werner, V., Baika, K., Fischer, P., Hadler, H., Obrocki, L., Willershäuser, T. et al. (2018) The sedimentary and geomorphological imprint of the AD 365 tsunami on the coasts of southwestern Crete (Greece) - examples from Sougia and Palaiochora. *Quaternary International*, 473, 66–90. Available from: https://doi.org/10.1016/j.quaint.2017.07.016

Williams, M.A.J. (2014) *Climate Change in Deserts: Past, Present and Future*. Cambridge University Press: New York. https://doi.org/10.1017/CBO9781139061780

Womack, W.R. & Schumm, S.A. (1977) Terraces of Douglas Creek, northwestern Colorado: an example of episodic erosion. *Geology*, 5(2), 72–76. Available from: https://doi.org/10.1130/0091-7613(1977)5<72:TODCNC>2.0.CO;2

Xoplaki, E., González-Rouco, J.F., Luterbacher, J. & Wanner, H. (2004) Wet season Mediterranean precipitation variability: influence of large-scale dynamics and trends. *Climate Dynamics*, 23(1), 63–78. Available from: https://doi.org/10.1007/s00382-004-0422-0

How to cite this article: Macklin, M.G., Booth, J., Brewer, P.A., Tooth, S. & Duller, G.A.T. (2022) How have Cretan rivers responded to late Holocene uplift? A multi-millennial, multi-catchment field experiment to evaluate the applicability of Schumm and Parker's (1973) complex response model. *Earth Surface Processes and Landforms*, 1–20. Available from: https://doi.org/10.1002/esp.5370